Understanding Interannual Groundwater Variability in North India using GRACE

GURU PRADHAN
March, 2014

ITC SUPERVISOR
Dr. Rogier van der Velde

IIRS SUPERVISORS
Dr. P.K. Champati Ray
Mr. Suresh Kannaujiya

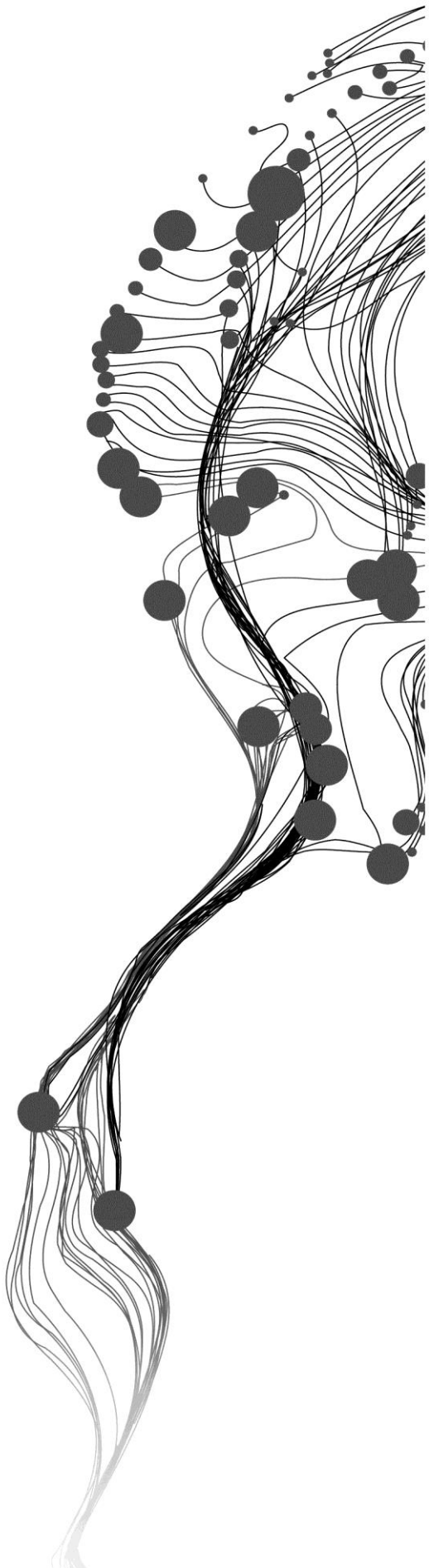

Understanding Interannual Groundwater Variability in North India using GRACE

Guru Pradhan
Enschede, the Netherlands [March, 2014]

Thesis submitted to the Faculty of Geo-information Science and Earth Observation of the University of Twente in partial fulfilment of the requirements for the degree of Master of Science in Geo-information Science and Earth Observation.

Specialization: Natural Hazards and Disaster Risk Management

THESIS ASSESSMENT BOARD:

Chairperson : Dr. V.G. Jetten
External Examiner : Dr. Rajesh S., (WIHG, Dehradun)
ITC Supervisor : Dr. Rogier van der Velde
IIRS Supervisor : Dr. P.K. Champati Ray
IIRS Supervisor : Mr. Suresh Kannaujiya

OBSERVERS:

ITC Observer : Dr. N.A.S. Hamm

FACULTY OF GEO-INFORMATION SCIENCE AND EARTH OBSERVATION, UNIVERSITY OF TWENTE, ENSCHEDE, THE NETHERLANDS

INDIAN INSTITUTE OF REMOTE SENSING
Indian Space Research Organisation
Department of Space, Government of India

DISCLAIMER

This document describes work undertaken as part of a programme of study at the Faculty of Geo-information Science and Earth Observation (ITC), University of Twente, The Netherlands. All views and opinions expressed therein remain the sole responsibility of the author, and do not necessarily represent those of the institute.

"When the well is dry, we know the worth of water."

- Benjamin Franklin

"For all of its uncertainty, we cannot flee the future"

- Barbara Jordan

"Uncertainty and mystery are energies of life. Don't let them scare you unduly, for they keep boredom at bay and spark creativity."

- R.L. Fitzhenry

ABSTRACT

Though groundwater stress in North India has been extensively studied in the past with the help of the Gravity Recovery and Climate Experiment (GRACE) satellite mission, interannual variability of groundwater storage (GWS) in the region remains unexplored. Higher variability denotes more uncertainty and volatility, and an uncertain groundwater supply can lead to unexpected shortfalls during periods when water is needed the most. From January 2003 to December 2012, GWS depletion rate was found to be approximately -1.6 ± 0.04 cm yr^{-1} in the area roughly corresponding to the Indian side of the Indo-Gangetic plains which translates into about 160 km^3 of net groundwater loss – equivalent to more than sixteen times the active capacity of India's largest dam reservoir. In the Indus and Ganges Basins, the groundwater depletion rate has slowed down remarkably compared to previous studies but there are still respective net groundwater losses of 60 km^3 and 100 km^3 over the 10-year study period. Furthermore, groundwater depletion was found to be particularly pronounced near the Himalayan inter-plate collision zone suggesting leakage of tectonic and erosion-driven mass loss signals into the GWS solution.

The interannual standard deviation of groundwater was found to be 1.5 ± 0.1 cm, which translates into a projected 95% confident yearly regional groundwater shortfall of 34 km^3. This unexpected deficit can be particularly devastating during a dry year. Moreover, the Gangetic basin was found to have a higher interannual standard deviation than the Indus Basin indicating higher groundwater variability in the former. Subsequently, this work went on to study the time evolution of interannual GWS variability and detected a non-negligible rise in the 12-month moving standard deviation over North India of 0.12 ± 0.04 cm yr^{-1}. This suggests that regional GWS variability is on the rise. The interpretation of this development is difficult but increased monitoring of groundwater in the region is warranted as this change might be a precursor to a fundamental shift in the regional groundwater system.

The GRACE-derived GWS values agree reasonably well with *in situ* well observations with correlation of 0.80 ± 0.03 and R-Squared of 0.64 ± 0.05 over a part of Uttar Pradesh thus supporting the validity of this remote sensing approach. The RMS error between the GRACE and *in situ* GWS time series was 8.43 ± 0.53 cm which is quite high however considering inherent uncertainties in the *in situ* data this study considers this margin of error reasonable. This work concludes that rapid, accurate regional GWS mapping is possible through the GRACE mission. In light of continued groundwater depletion and possible increase in GWS variability over North India, this study advocates for more robust water conservation and storage measures.

Keywords: *GRACE, GLDAS, Groundwater, Northern India, Interannual Variability, CGWB, Depletion, Water Security, Hydrology, Well, Empirical Bayesian Kriging*

ACKNOWLEDGEMENTS

This work could not have been possible without the help of many sources – both human and digital! Countless people have contributed directly or indirectly in the completion of this thesis and I thank you all from the bottom of my heart! Please do not feel offended if you don't find your name explicitly mentioned here – you are still important!

I would like to express my deepest gratitude to Dr. Y.V.N. Krishna Murthy (Director, IIRS), Dr. S.P.S. Kushwaha (Group Director, PPEG), Dr. P.L.N Raju (Group Head, Geoinformatics), Dr. S.K. Saha (Group Head, Earth Resources and Systems) for facilitating my transition from Post-Graduate Diploma to the Masters of Science program. Countless thanks to my supervisors in Indian Institute of Remote Sensing and University of Twente – Dr. P.K. Champati Ray, Dr. Rogier van der Velde, Mr. Suresh Kannaujiya – for the constant encouragement and crisp, indispensable feedback.

Of course, I am indebted to the faculty and research fellows from each academic department at IIRS who gave me a brief but insightful introduction to topics and matters in fields ranging from marine & atmospheric systems to urban information systems. I also extend my sincere gratitude to the instructors and research fellows who enlightened me in the advanced modules and coursework at University of Twente.

Now, a word of appreciation to my classmates, seniors, and friends at IIRS and UT; there are far too many of you to mention but I will try anyhow. Raj B., Colonel Sir, Ishaan, Kanishk, Aravind, Piyush, Abhisheikh S., Tanya, Akhil, Apoorva, Neha, Hemlata, Ravisha, Amit, Shreya, Girija, Sahil, Pradeep – it is a good MSc. group we got, we will stay in touch. Unmesh, Parag, Amit Sir, Shashi G., Anant, Hemanthi, Ponraj, Sai K., Bond, Shishant, Soumya, Joyson, Akanksha, Vivek – my MTech. comrades, it was a pleasure. Special mention goes to Rohit, the best roommate out there, and Taibang for his gracious hospitality and expert culinary skills. My long-departed PG Diploma friends – Kelhou, Priyanka, Rosmary, the Rafaels, Oswaldo, David, Ramanuj, Vedika, Ritanjali, Manish Sir, Gangesh, Himanshu, Tarun, Moa, Azzedine, Tamrat, Preeti, Anil, Blecy – miss you all and hope you are doing well. My ITEC compatriots – Dorji, Daniel, Jasneel, Menuka, Angela, Sabin, Calvin, Sherzhod, Thabo, Eduardo, Ganessan, Ajit, Tia – we shall meet again. Friends at UT – Zelalem, Raghudeep, Iria, Twang, Franklin, Payam, Mehdi, Sidhi, Gunamani, Rahul Raj – it was fun!

Space is short so I will list the remaining folks here. Thank you all! My parents and extended family, librarians, administrative staff, mess members, security staff, cleaning staff, Lucy the campus pet dog. Special mention to my juniors (especially the Kolaveri Club) – you are in good hands!

TABLE OF CONTENTS

LIST OF FIGURES

LIST OF TABLES

1. INTRODUCTION

1.1. Background

North India has earned the unenviable distinction of being one of the most water stressed regions in the world ("India among high risk nations in water stress survey," 2013). With a population exceeding 500 million people, the region's agriculture and food security is heavily reliant on groundwater-based irrigation to feed its large yet booming population. The combination of climate change, large-scale contamination of shallow groundwater resources (Nahar, Hossain, & Hossain, 2008), and the planned diversion of surface water resources from the Northern regions to the dryer Southern regions (Misra et al., 2006) all serve to intensify an already deteriorating water security situation. Furthermore, recent regional groundwater mapping of North India using Gravity Recovery and Climatology Experiment (GRACE) satellite observations and Global Data Assimilation System land surface models (see Chapter 2 for more detailed discussion regarding measurement of GWS) have all unanimously shown unsustainable groundwater depletion trends (Gleeson et al., 2012; Rodell et al., 2009; Tiwari et al., 2009). Though these findings helped quantify and illuminate the worsening groundwater scenario, they have not fully exploited the immense information contained within the GRACE-derived groundwater storage (GWS) time series.

This study has multiple overlapping goals which ultimately link to a better understanding of the interannual groundwater variability over North India from 2003 till 2012. The first goal is to re-calculate and update the groundwater depletion trend (if any) across the North Indian region to assess any shifts or changes in regional groundwater activity with respect to GRACE estimates from previous studies. The work then moves beyond the GWS trend analysis and explores the interannual variability of groundwater over North India. This will be achieved by first quantifying the level of year-to-year variability across the region and then studying the time evolution of yearly GWS variability to identify possible shifts in regional groundwater dynamics over the 10-year study period. Another novel aspect of this research is the validation of *in situ* well data with GRACE observations over a part of the Indian state of Uttar Pradesh.

Interannual variation of GWS measures the variability of groundwater levels at time scales of one (1) year or longer. Groundwater fluctuations are driven by natural (rainfall, vegetation, soil types) and anthropogenic (socio-economic concerns, land use/land cover change, damming) processes with complex, non-linear interactions between them. Thus, one can expect to see a wide range of variability in yearly groundwater storage with some areas facing unexpected shortages or flooding. As such, interannual variability of GWS is a gauge of groundwater supply unpredictability and should be combined with mean GWS depletion rate to comprehensively measure water stress. Areas experiencing high interannual GWS variability face higher risk of water supply shortages even if there is little to no net loss of groundwater. In

the absence of adequate water governance and storage mechanisms, these supply shocks can be especially devastating during dry years (Reig et al., 2013). The level of yearly GWS variability can be captured by simply calculating the standard deviation of yearly average GWS in a manner similar to the one used to calculate interannual variation of sunlight over United States (Wilcox & Gueymard, 2010). More details on this can be found in Chapter 2.2.

This study also tackles the time evolution of GWS interannual variability over North India. Inspired by studies of shifts in river discharge variability, this work uses the moving standard deviation as the primary method to analyse the progression of yearly GWS variability (Booth et al., 2006). Even in areas where there is no net GWS change, any increase in GWS variability translates into higher frequency of extreme GWS behaviour (both high and low water tables), as well as an increase in the magnitude of these extreme events. Furthermore, a shift in the variability may be a precursor to fundamental changes in the groundwater – and perhaps underlying large-scale hydrological – dynamics which could lead to unexpected challenges that the region must contend with. An increase in GWS variability, combined with a negative trend in GWS levels, is even more worrisome. Such a development would denote lower water tables with more extreme drops in the water level which can have harsh implications for groundwater access and supply. The GWS depletion rates calculated during the course of this study will be combined with interannual variability results to better assess regional groundwater behaviour.

The final problem this thesis tackles involves the validation of the GRACE-derived GWS solution with well observations provided by Central Groundwater Board (CGWB), the primary authority for groundwater surveying and monitoring in India. Indeed, robust validation of the GRACE solution further reinforces the product's legitimacy for regional groundwater mapping applications. Due to both temporal and spatial undersampling of well observations, this work only considers selective validation of *in situ* data over the state of Uttar Pradesh. This research uses Empirical Bayesian Kriging (EBK), a relatively new geostatistical interpolation method to interpolate CGWB-derived GWS values. This novel approach corrects for and automates some model fitting difficulties inherent in classical kriging (Krivoruchko, 2012). Using datasets from the GRACE mission, the Global Land Data Assimilation System (GLDAS) land surface models, and CGWB; this thesis is a preliminary study of interannual variability of groundwater storage in the North Indian region.

1.2. Related Work

The regional analysis of groundwater depletion over North India using GRACE has been explored independently by both Tiwari et al. (2009) and Rodell et al. (2009) with both parties concluding that large-scale, unsustainable groundwater extraction is taking place (Rodell et al., 2009; Tiwari et al., 2009). This work was followed by a groundwater stress map or footprint of the Upper Ganges aquifer by Gleeson et al. (2012). Again, it was concluded that the region is undergoing widespread groundwater mining by using

a hydrological model and country/administrative unit water use statistics (Gleeson et al., 2012). All these works do well in characterizing first-order effects such as net depletion rates but they do not incorporate second-order effects such as the variability of the groundwater storage. Variability of groundwater storage translates into supply unpredictability which must be accounted for in water security assessments and met with adequate water storage and governance mechanisms (Reig et al., 2013).

A qualitative analysis of interannual variability of terrestrial water storage using GRACE has been explored over South Asia by tracking changes in the yearly average TWS values (Shum et al., 2010). The aforementioned study, however, does not focus on GWS and the study area encompasses a far larger area. Interannual variability of groundwater observation well data has been studied in Canada at three different regions using wavelet transforms and has shown remarkably different variability behaviours for each of the sites (Tremblay et al, 2011).

A coefficient of variation map has been prepared in many domains to quantify interannual variability for different phenomena: solar radiation (Wilcox & Gueymard, 2010), river discharge (Booth et al., 2006; Restrepo & Kjerfve, 2000), and NDVI (Milich & Weiss, 2000). After an extensive literature survey, no maps for interannual variability of GWS were found. The closest thing uncovered was the interannual variability map of total blue water detailed in the Aqueduct Water Risk Map (Reig et al., 2013). However, this map measures the interannual variability of available blue water which is essentially a measure of the runoff flowing into a catchment as measured from GLDAS simulations.

The main method for understanding and quantifying shifts in interannual GWS variability has been borrowed from literature rooted in climate change studies (Folland et al., 2002; Vinnikov & Robock, 2002). Folland et al. (2002) used extensive climatological datasets spanning nearly 100 years of observations and studied the probability distribution of both precipitation and temperature across different time periods to uncover any shifts in climate variability. Vinnikov and Robock, on the other hand, fit trends through the moments of various climatic indices to determine whether the observed climate is getting more or less variable. Vinnikov and Robock's approach is adopted in this thesis to test for shifts in GWS variability.

Validation of the GRACE-derived groundwater storage solutions have been carried out successfully over areas as diverse as Mississippi River Basin (Rodell et al., 2006), Bangladesh (Shamsudduha et al., 2012), and Yemen (Moore & Fisher, 2012) over study areas exceeding 200,000 km^2. As of now, no extensive validation of GRACE has been carried out over India using *in situ* well observations. Additionally, whenever efforts to validate GRACE results have been carried out, they have all used simple averaging of in situ well data or deterministic interpolation techniques such as inverse distance weighing (IDW) or Thiessen polygons to derive gridded GWS outputs. This is contrary to the rich and diverse literature all

concurring with the effectiveness of geostatistical methods (kriging) for hydrological applications – especially with interpolation of groundwater data (Ahmadi & Sedghamiz, 2006; Delbari et al., 2013; Machiwal et al., 2012). Even then, these studies all use ordinary kriging methods where several theoretical semivariograms (spherical, exponential, circular etc.) are used to model the actual or empirical semivariogram. The semivariogram model that best fits the empirical semivariogram is then assumed to be the true semivariogram without taking into account fitting errors. This study departs from previous kriging efforts by using Empirical Bayesian Kriging in order to correct for this fitting problem.

1.3. Research Identification

1.3.1. General Objective

This study aims at quantifying and understanding interannual variability of groundwater storage over the North Indian states of Bihar, Haryana (including Delhi NCR), Punjab, Rajasthan, Uttar Pradesh, and West Bengal for the time period encompassing January 2003 till December 2012. Better understanding of interannual GWS variability would require derivation of groundwater depletion rates (if any) and also validation of GRACE data with *in situ* well observations to bolster the legitimacy of this remote sensing approach.

1.3.2. Sub-Objectives

The successful accomplishment of the research objective requires that the following sub-objectives be met:

- To estimate the GWS and its rate of change in the North Indian region from 2003 till 2012, and compare with previous works on the same subject
- To compute the interannual standard deviation both at the pixel (1° x 1°) and regional level in order to quantify interannual GWS variability
- To detect any change in interannual GWS variability in North India during the period 2003-2012
- To validate *in situ* well observation data with GRACE-derived GWS solution for the state of Uttar Pradesh using Empirical Bayesian Kriging

1.3.3. Research Questions

The study will attempt to answer the following research questions:

1) How is GWS estimated from GRACE and GLDAS observations?

2) What is the level of uncertainty associated with the GRACE-derived GWS results and how do these errors propagate?
3) How is GWS estimated from *in situ* well observations?
4) What criteria are to be used to enable effective comparison between GRACE and CGWB-derived GWS solutions?
5) What can the interannual standard deviation say about groundwater dynamics in the study region?
6) Can information regarding GWS depletion rate and time evolution of groundwater variability be used to shed light on regional water stress, and what might be effective ways to combat it?

1.4. Thesis Structure

The research work is organized as follows:

Chapter 1: *Introduction* – the concept of groundwater interannual variability is introduced and the thesis's motivation is described. The research objectives of this study and the research questions that are to be answered are furthermore presented along with previous work carried out.

Chapter 2: *Theoretical Background* – this section deals with the derivation of GWS using the Water Balance Method from GRACE Terrestrial Water Storage (TWS) measurements and GLDAS hydrological outputs. The concept of interannual variability and measurement of shifts in variability is then displayed. Subsequently, there is an introduction to the GRACE satellite mission, the GLDAS project, and the CGWB well data. Then, the importance of error and uncertainty propagation is expanded upon, and the use of Monte Carlo methods is commented upon. The chapter ends with the literature review.

Chapter 3: *Study Area* – the climatic, hydrogeological, agro-economic context of the North Indian region is dealt with in this chapter.

Chapter 4: *Data and Methods* – this chapter deals with the datasets used in the course of this research. A short description regarding the GRACE, GLDAS, and CGWB datasets is given and is followed by the software used. Various techniques utilized for processing GRACE, GLDAS, CGWB datasets are explained in detail: Trend Analysis, Time Series Decomposition, Monte Carlo Method, Calculation of Interannual Standard Deviation, Moving Statistics, Regional Analysis, Well Data Processing, and Empirical Bayesian Kriging.

Chapter 5: *Results and Discussion* - the interannual variation level across North India is discussed and then followed by results regarding changes in interannual GWS variability. Subsequently, the validation efforts are analysed and the accuracy of GRACE is commented upon.

Chapter 6: *Conclusion and Recommendations* – the final section provides conclusions and recommendations for future work along with some advice for policymakers.

2. THEORETICAL BACKGROUND

2.1. Remote Sensing Tools and Land Surface Modelling

Answering the research questions required the use of the GRACE Level 3 Processed Terrestrial Water Storage (TWS) solutions and the land surface model outputs from GLDAS. A short description of both these datasets is outlined below.

2.1.1. GRACE Mission

The Gravity Recovery and Climate Experiment (GRACE) is unprecedented in that it is the first satellite remote sensing mission directly applicable for regional groundwater mapping (Rodell et al., 2006) though its primary directive is to obtain accurate estimates of Earth's gravity field variations (Tapley et al., 2004). The mission consists of two satellites flying in tandem in a polar, near circular orbit at 500 km altitude with an inter-satellite separation distance of approximately 220 km. The gravity field information is actually inferred from the inter-satellite distance which is measured within μm accuracy using a K-Band microwave system (Tapley et al., 2004). Potential error sources such as atmospheric drag and satellite perturbations are measured and filtered out using readings from a highly accurate, on-board accelerometer while precise positioning is determined using on-board GPS receivers (Tapley et al., 2004).

The principal and admittedly unconventional idea behind GRACE is that the satellites themselves act as the principal measurement devices. The two satellites (also known as 'Tom' and 'Jerry') work in tandem to map the gravitational field of the Earth. When surface features that distort the gravitational strength such as mountains (which decrease the gravitational field strength) are encountered, the leading satellite accelerates by a certain amount followed by the trailing satellite which then catches up (see figure 2.1). These minute changes in the inter-satellite distance are then fed into what are essentially massive regression engines in order to determine the gravity field strength at the data processing facilities in Jet Propulsion Laboratory (JPL), University of Texas – Austin Centre for Space Research (CSR), and the GeoForschungZentrum (GFZ).

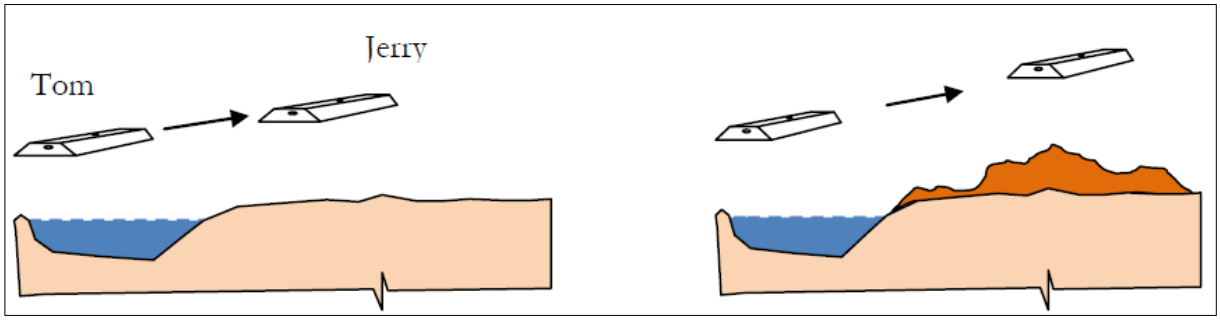

Figure 2-1: The inter-satellite distance varies according to the local gravitational anomaly. When the leading satellite encounters a land/sea interface (left), it decelerates due to the higher gravitational pull because of the denser oceanic crust. On (right), mountainous regions have lower gravitational strength due to isostasy so the inter-satellite distance increases as the leading satellite accelerates (Haile, 2011).

At the data centres, the K-Band Level-1 radar data is converted into gravitational field information in the form of spherical harmonic coefficients (Rodell et al., 2006; Wahr et al., 1998). These coefficients are available as Level-2 products and have been corrected for atmospheric and oceanic circulation, and solid Earth tides using underlying models (Rodell et al., 2006).

Water is quite heavy and is usually the largest contributor to mass variability on the earth's surface (Ogawa, 2010). By assuming that gravity changes are primarily driven by changes in distribution of terrestrial water storage, the Level-2 spherical harmonics data can be further processed to express the gravity field changes in terms of 'equivalent water thickness' (Ogawa, 2010). The term 'equivalent water thickness', or EWT, is derived from the assumption that these hydrological mass changes are concentrated in a very thin layer on the Earth's surface (Wahr et al., 1998) whose vertical extent is measured in centimetres (see fig 2.2). Changes in EWT are available as Level-3 Terrestrial Water Storage (TWS) solutions after further filtering and correction for post-glacial rebound. This dataset provides the ΔTWS values needed for the water balance equation detailed in equation (2.1) and (2.2). Furthermore, this processing limits the accuracy of TWS observations to be valid only for large geographical areas exceeding 200,000 km^2.

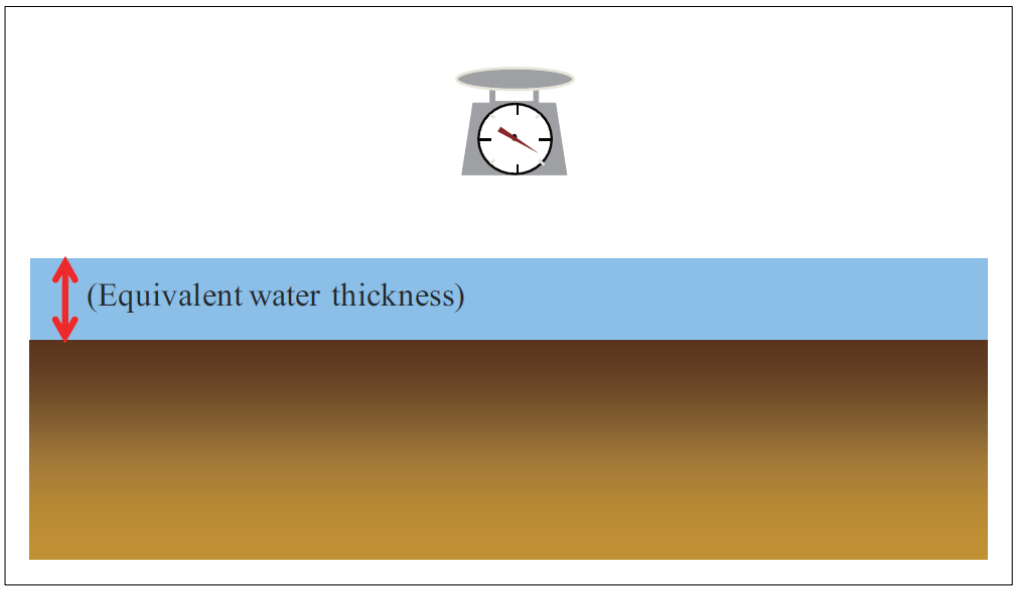

Figure 2-2: Visualization of equivalent water thickness (EWT). Note that the terrestrial water storage is assumed to be concentrated in a very thin layer on the Earth's surface (Ogawa, 2010)

2.1.2. GLDAS

The Global Land Data Assimilation System (GLDAS) is an inter-institutional effort undertaken by National Aeronautics and Space Administration (NASA) and National Oceanic and Atmospheric Administration (NOAA) in order to simulate land surface state (soil moisture, surface temperature) and flux (evapotranspiration, sensible heat flux) parameters globally at high spatial resolution and in a near real-time basis (Rodell et al., 2004). As such, it drives four (4) offline (uncoupled with atmosphere) land surface models, assimilates an enormous amount of satellite and ground-based observations, and produces outputs at resolutions ranging from 0.25° to 1°. The land surface models being driven by GLDAS are: NOAH, MOSAIC, Community Land Model (CLM), and Variable Infiltration Capacity (VIC). The principal advantage of GLDAS is its sophisticated data assimilation engine which ingests vast amounts of remote sensing and *in situ* observations in a near real-time fashion in order to constrain land surface model outputs from deviating too far from observed states. The $\Delta SM, \Delta SWE, \Delta\mathrm{CWS}$ components of the water balance equation detailed in section (2.3) of this chapter are obtained using GLDAS land surface model simulations.

2.2. *In Situ* Well Data

This study has access to data from 3597 monitoring wells scattered across the Indian states of Delhi NCR, Haryana, Rajasthan, and Uttar Pradesh kindly provided to us by Central Groundwater Board (CGWB). Initially, most of the CGWB well observation system consisted of dug wells. However, these are being gradually replaced by piezometers for water level monitoring with measurements generally

being taken four times a year in the months of January, April/May, August, and November (Jain & Singh, 2003). Recently, automated measurement systems are being installed in select wells that would enable real-time monitoring of groundwater levels however nationwide implementation is yet to take place (Goswami, 2014).

Even though the guidelines stipulated quarterly observation of groundwater levels, the periodicity of these measurements vary state to state, and from site to site (Central Ground Water Board, 2011). Accordingly, the CGWB datasets were subject to systematic quality control procedures to screen out well records with large temporal gaps, missing records, or insufficient observations. Subsequently, the short-listed well time series were converted into groundwater storage changes, and then gridded to the same spatial resolution as the GRACE Level-3 TWS solution. Furthermore, the CGWB well data was processed only for the state of Uttar Pradesh in order to selectively validate the GRACE solutions. A detailed description and rationale of this methodology is described in Chapter 4.

2.3. Estimation of Groundwater Storage Change Using Water Balance Approach

Estimation of groundwater storage (GWS) at a regional scale can be approximated through the use of the water balance equation. A water balance approach is a fundamental hydrological technique which states that the flow of water into and outside of a system must equalize or 'balance' (Rodell et al., 2006) with the change in storage. Accordingly, the water balance method to compute terrestrial water storage changes in the North Indian region can be expressed as:

$$\Delta TWS = \Delta SM + \Delta GWS + \Delta SWE + \Delta CWS + \Delta SW \quad (2.1)$$

Where $\Delta\mathrm{TWS}$ is the change in terrestrial water storage, $\Delta\mathrm{SM}$ is the change in soil moisture, $\Delta\mathrm{GWS}$ is the change in groundwater storage, $\Delta\mathrm{SWE}$ is the change in snow-water equivalent, $\Delta\mathrm{CWS}$ represents the change in canopy storage, and $\Delta\mathrm{SW}$ is the change in surface water storage. All the above parameters are expressed as centimetres of equivalent water thickness (EWT). Re-arranging equation (2.1) in context of the GRACE-derived Level 3 (L3) $\Delta\mathrm{TWS}$ estimates, the GLDAS-based land surface model outputs of soil moisture ΔSM , snow-water equivalent $\Delta\mathrm{SWE}$, and canopy storage $\Delta\mathrm{CWS}$, and assuming that surface water change is negligible; we can calculate change in groundwater storage as:

$$\Delta GWS = \Delta TWS - \Delta SM - \Delta SWE - \Delta CWS \quad (2.2)$$

The GRACE L3 solution vertically integrates all sources of hydrological variability as well as other unaccounted sources such as earthquakes (Mikhailov et al., 2004) and other residuals. The decision to

discount surface water change stems from the general observation that surface water can be considered as the intersection of the water table with the land surface (Winter, 1999). Since the approach taken in equation (2.2) assumes that groundwater is spatially continuous across the area of interest, surface water can be considered as an extension of groundwater and can be removed from the water balance equation. Still, this assumption fails during times of extreme flooding and in very moist regions of the world such as the Amazon (Rodell et al., 2006). Nevertheless, as a general approximation for GWS, equation (2.2) holds value and is used in this thesis.

2.4. Interannual Variability of Groundwater Storage

Studying GWS variability is often confounded by the presence of seasonal and trend components. These factors often exaggerate or dampen the actual variability of the time series so they must be removed in order to properly isolate the variability of the groundwater levels (Zhang & Qi, 2005). The raw GWS time series must be de-seasonalized and detrended (see section 4.5) in order to isolate the groundwater storage variations. Subsequently, the task of quantifying and detecting shifts in GWS interannual variability can be undertaken.

2.4.1. Interannual Standard Deviation

In order to quantify the level of year-to-year volatility in GWS levels, the interannual standard deviation is computed both at the pixel and the regional level. The interannual standard deviation is derived in a manner similar to Wilcox & Gueymard, (2010) and will retrieve the mean annual GWS over the 10-year period $< \mathrm{GWS} >$ and the average annual GWS value $\mathrm{GWS_i}$ for each specific year i to calculate the interannual standard deviation using the following formula:

$$\sigma = \sqrt{\left[\frac{1}{10}\sum_{i=1}^{10}(< GWS > - GWS_i)^2\right]} \tag{2.3}$$

The result of equation (2.3) will express the general level of dispersion around the mean yearly, long-term groundwater storage level. It is a measure of the volatility of the groundwater supply and conveys the likelihood of data falling within σ around the mean. Assuming a normal distribution of GWS, one can be reasonably or 68% confident that the mean yearly GWS level will be within one σ around the long-term mean. However, when designing robust water management policies it makes sense to work with 95% confidence intervals and make allowances that yearly mean GWS levels may fluctuate by $\pm 2\sigma$ from the long-term average. The higher the interannual standard deviation, the larger the likelihood of extreme swings in GWS levels on a year-to-year basis. This is, of course, a simplification as groundwater varies in complex ways in response to external stimuli however the interannual

standard deviation can serve as a useful approximation of yearly GWS volatility and as a rough tool for making yearly groundwater shortfall projections.

2.4.2. Shift in Interannual Groundwater Storage Variability

It is important to differentiate between changes in the mean GWS levels (which are approximated through trend analysis) and changes in GWS variability. Changes in GWS variability can be thought as the change in the range of the highest and lowest GWS levels (Hiraishi et al., 2000). Thus, an increase in GWS variability translates into an increase in the frequency of both extreme high and low water table fluctuations, as well as an amplification of the magnitude of these events. Though there has been a lot of emphasis on declining groundwater levels, extremely high water tables are just as disruptive. If the water table rises to the surface, one can expect flooding of urban areas, waterlogging and salinization of agricultural fields, and more amenable conditions for growth of pests such as mosquitoes, ticks, locusts, rodents etc. (Kovalevsky, 1992). Thus, it is of immense value that any shifts in GWS variations are understood and accounted for when implementing water storage and distribution schemes. Figure 2-3 demonstrates different scenarios involving changes in the groundwater regime and their effects on the water table.

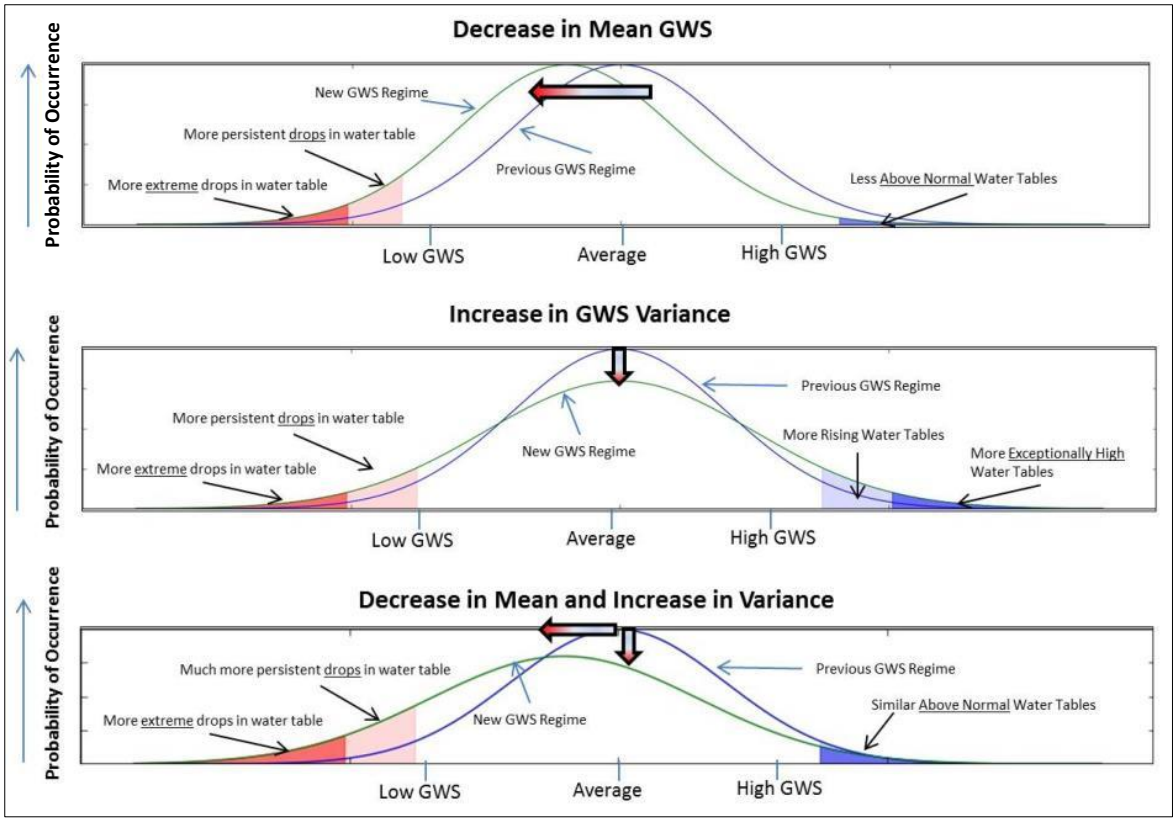

Figure 2-3: Schematic for visualizing effects on extreme GWS events in different scenarios

The methodology adopted to identify shifts in GWS interannual variability is quite a simple one and involves the use of moving statistics. Inspired by the use of moving standard deviation for detecting shifts in streamflow variability in the hydrological community (Booth et al., 2006), a simple 12-month moving standard deviation is passed over the GWS time series to identify any shifts in the yearly standard deviation. The moving standard deviation is calculated for an arbitrary window size w in the following manner:

$$\hat{\sigma}_t = \begin{cases} \sqrt{\frac{1}{w}\left(\frac{1}{2}\left(X_{t-q} - \hat{m}_t\right)^2 + \left(X_{t-q+1} - \hat{m}_t\right)^2 + \cdots + \frac{1}{2}\left(X_{t+q} - \hat{m}_t\right)^2\right)} \; for\; w = 2q, q < t < n - q, \\ \sqrt{\frac{1}{w}\left(\left(X_{t-q} - \hat{m}_t\right)^2 + \left(X_{t-q+1} - \hat{m}_t\right)^2 + \cdots + \left(X_{t+q} - \hat{m}_t\right)^2\right)} \; for\; w = 2q+1, q+1 < t < n + q. \end{cases} \quad (2.4)$$

Where $\hat{m}_t$ is the simple moving average at time t and n is the last time index value recorded. Similar methods can be extended to calculate the moving skewness and moving kurtosis of a time series. A 12-month running skewness window will track changes in skewness of the dataset and can be used to detect changes in direction of extreme events (Doane & Seward, 2011). For example, an increase in skewness for GWS anomalies suggests a longer right-tail. Incidentally, a right-tailed distribution indicates a larger tendency towards positive GWS values and an uptick in the frequency of higher than normal water tables thus leading to more urban flooding events, waterlogging etc. Similarly, a decreasing skewness suggests a propensity towards negative GWS events as well as in the number of extreme negative GWS anomalies.

A 12-month moving kurtosis window will detect shifts in yearly kurtosis – a statistical measure of how heavy tailed a random variable is (DeCarlo, 1997; "SAS Elementary Statistics Procedure," 2008). High kurtosis signifies that a large portion of the overall variance is due to a few extreme events. A lower kurtosis, on the other hand, suggests a more uniform distribution with the variance primarily driven by a large number of small- to medium-sized deviations from the mean.

2.5. Error Propagation

No scientific analysis, model, or simulation is complete without accounting for uncertainty in the raw datasets, and its propagation through intermediate and final calculations. The GRACE Level-3 TWS datasets have significant measurement and leakage (from oceans and surrounding pixels) errors associated with each pixel. Different land surface model outputs for the same variable and for the same location may vary considerably due to different modelling approaches, algorithm implementations, and soil layer parameterisations (Rodell et al., 2004). The error propagation analysis of *in situ* well observations is even

more challenging due to temporal undersampling of the readings, and mischaracterization of aquifer properties. In this thesis, the error propagation scheme adopted is to express the uncertainty of a hypothetical, measured variable x as its standard deviation σ_x so the final value of the variable and its associated error is defined as $(x \pm \sigma_x)$. If variable x follows a normal distribution, then one can be 68% or 'reasonably' certain that the true value of x lies within one $\pm\sigma_x$ (standard deviation) from the recorded value of x. Similarly, one can be 95% or 'strongly' confident that the real value of x lies in the region bounded by$(x \pm 2\sigma_x)$.

What follows is a short explanation of the principal uncertainty propagation techniques used in this work to compute uncertainties at each intermediate step all the way to the final results. First-order error propagation methods were used to compute uncertainties involving simple and straightforward calculations whereas Monte Carlo methods were resorted to in the case of more complex and nonlinear interaction of variables.

2.5.1. First-Order Error Propagation

Computation of uncertainty for simple arithmetic operations can be well approximated through first order error propagation formulae without recourse to the computationally intensive Monte Carlo simulations. Table 2.1 shows how to compute the standard deviation or uncertainty for simple operations. Here, X, Y represent the variables being operated on with standard deviations (errors) σ_X, σ_Y respectively. a, b represent known scalar constants, and it is assumed that both X, Y are uncorrelated.

Table 2-1: First Order Error Propagation Approximation Formulae (Hiraishi et al., 2000)

Operation	Uncertainty
$Z = aX \pm b\,Y$	$\sigma_Z = \sqrt{a^2\sigma_X^2 + b^2\sigma_Y^2}$
$Z = XY$	$\sigma_Z = Z\sqrt{\frac{\sigma_X^2}{X^2} + \frac{\sigma_Y^2}{Y^2}}$
$Z = X/Y$	$\sigma_Z = Z\sqrt{\frac{\sigma_X^2}{X^2} + \frac{\sigma_Y^2}{Y^2}}$

$Z = X^a Y^b$	$\sigma_Z = Z\sqrt{\left(\frac{a\sigma_X}{X}\right)^2 + \left(\frac{b\sigma_Y}{Y}\right)^2}$

2.5.2. Monte Carlo Method

Uncertainty analysis involving complex, nonlinear interaction between multiple variables cannot be well captured by first-order, linearized error propagation calculations. In this case, Monte Carlo analysis can be used to treat source variable uncertainties (Hiraishi et al., 2000). Simply put, Monte Carlo methods work in the following manner to provide bounds or distributions to an output function (Smith, 2006):

1) Choose a distribution that describes possible values of a parameter.
2) Generate synthetic data drawn randomly from this distribution.
3) Utilize the generated data as possible values of the input parameters to produce an output state space.
4) Study the distribution of the results in order to compute uncertainty. If the output is normally distributed or can be well approximated with a normal distribution, the mean value serves as the final output variable with the standard deviation as the uncertainty associated with the final result.

This study makes full use of Monte Carlo methods to generate synthetic GWS time series and explores the possible state space of both the intermediate and final results. For simple averaging and other operations, first-order error approximation techniques were instead implemented. In the case of Monte Carlo simulations, the information contained in the distribution of the output variables is then used to compute the resultant value and the uncertainty associated with it. More details about this procedure are contained in Chapter 4.

3. STUDY AREA

3.1. Background

The study area encompasses the Indian states predominantly located in the densely populated, heavily irrigated Indo-Gangetic plains. This region contains the states of Bihar, Haryana (including Delhi NCR), Punjab, Rajasthan, Uttar Pradesh, and West Bengal (see Fig 3-1). As of the Indian Census of 2011 (Chandramouli, 2011), the combined population of these states is around 530 million people and rising. The state of Rajasthan indeed does not fall entirely into the Indo-Gangetic plains region except for its northern and eastern region but has been included in this study area as well. Lying between 68.2°-89.1° E Longitude, 24.3° - 32.2° N Latitude, the Indian portion of the Indo-Gangetic plains consists of the large floodplains of the Ravi, Beas, Sutlej, and Ganges Rivers, and are underlain by thick piles of Tertiary and Quaternary sediments (Jha & Sinha, 2009). This thick pile of alluvial deposits, which exceed 1000 meters in thickness at some locations, is extremely fertile and forms the largest consolidated area of irrigated food production in the world with a net cropped area of 114 million hectares (B. R. Sharma, Amarasinghe, & Sikka, 2008). Indeed, more than 90% of the total water use in the area is for agriculture, with 8% followed by domestic use (B. Sharma et al., 2008).

Figure 3-1: Political map of India with the study area states labelled ("Political Map of India," 2012)

Though the Indo-Gangetic plains region has a substantial surface-based irrigation infrastructure in place, groundwater-based irrigation is currently the favoured system for watering crops (B. Sharma et al., 2008).

In fact, it is extremely difficult to find a farmer who either does not have his own pump or does not purchase water from the neighbouring pump owner (Jain & Singh, 2003). Groundwater pumping is one of the major driving forces behind the 'green revolution' of the 1970s which brought irrigation to areas not covered by surface irrigation, and helped catapult India from a nation reliant on food imports to a net food exporter (Shah, Roy, Qureshi, & Wang, 2003). The large-scale pumping of groundwater that fuelled the agricultural transformation has however led to increasing land and water degradation, water logging and salinization in highly irrigated areas, pollution of water resources, and declining water tables which all pose a grave threat to the water and food security of India.

3.2. Agriculture

Major crops grown in the study area are rice, wheat, cotton, millet, maize, and sugarcane which are grown in a dual cropping scheme: rice during the *rabi* period (October-March) and wheat during the *kharif* period (July-October) (Washington et al., 2012). Regional agricultural characteristics are detailed in Figure 3.2 with the western sub-regions 1, 2, and 3 (which roughly correspond to the states of North Rajasthan, Punjab, Haryana, Delhi NCR, Western U.P.) being a food surplus region featuring high productivity, high investment, and heavy use of groundwater for irrigation. In contrast, the eastern sub-regions 4, 5 (Eastern U.P., states of Bihar and West Bengal) form a largely food deficit region with low productivity, higher flood hazard risk, and poorer infrastructure (Aggarwal, Joshi, Ingram, & Gupta, 2004).

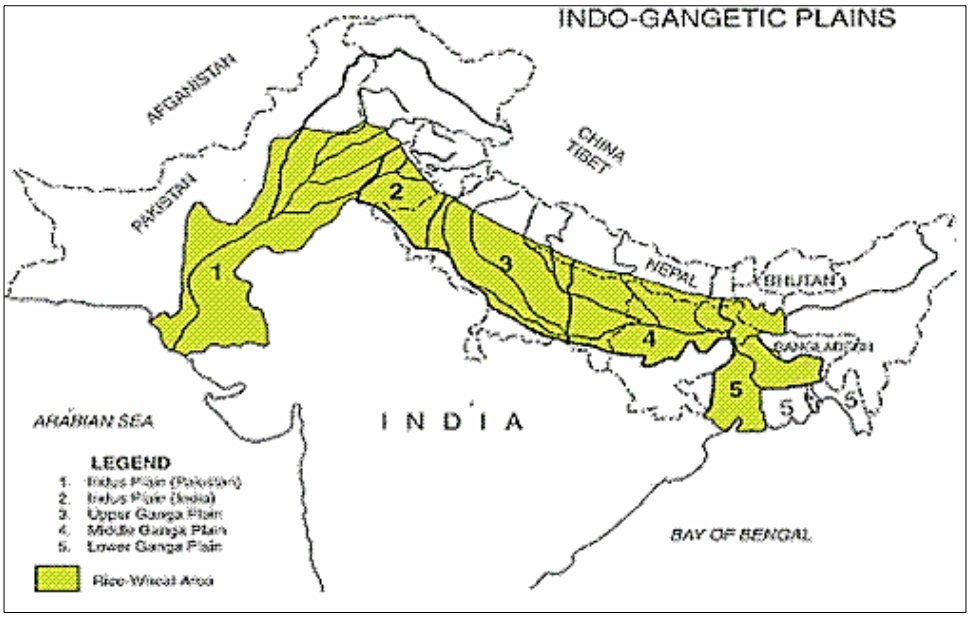

Figure 3-2: Agriculture zone map of Indo-Gangetic Plains (Aggarwal et al., 2004)

3.3. Climate

It is quite a challenge to generalize the climate of such a large study area however one can divide it into four seasons: Winter (December – April), Pre-Monsoon (April – June), Monsoon (June – September), and Post-Monsoon (October – December) (Sehgal, Singh, Chaudhary, Jain, & Pathak, 2013). The main source of rainfall in the region is the Southwest Monsoon which is known to account for 70-90% of the total annual rainfall over India (Rajeevan & McPhaden, 2004). Depending on the strength of the monsoon, typical annual rainfall over upper Indo-Gangetic Plains (Punjab, Haryana, North Rajasthan, and Western Uttar Pradesh) is 550 mm whereas lower Indo-Gangetic Plains (Eastern Uttar Pradesh, Bihar, West Bengal) is 1200 mm (Sehgal et al., 2013). However, this rainfall is unevenly distributed across the region with the dry Thar Desert in Rajasthan receiving less than 250 mm of rain in a year, and heavy rainfall being observed in parts of West Bengal to the tune of 2500 mm in a year (Central Ground Water Board, 2011).

3.4. Hydrogeology

The Indo-Gangetic plains are underlain with an extensive layer of Quaternary alluvial deposits, and bordered by the Himalayan mountain range to the north and the Deccan Shield to the south (Central Ground Water Board, 2011). The hydrogeological map of India is shown below in Figure 3-3. The region's hydrogeology can be divided into three distinct, unconsolidated regions (Bhabar, Terai, Central Ganga Plains).

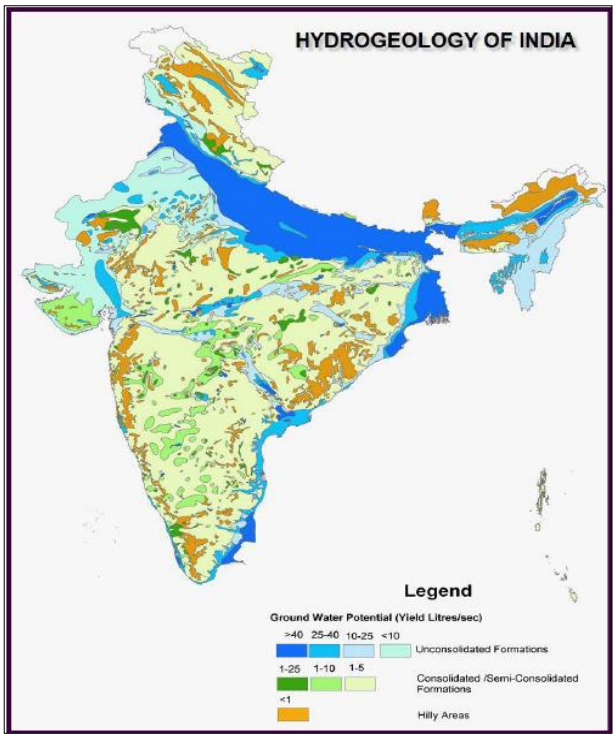

Figure 3-3: Hydrogeological Map of India (Central Ground Water Board, 2011)

Bhabar Belt: Lying near the Himalayan foothills and confined to the northern parts of Punjab and Uttar Pradesh, the Bhabar Belt consists most of coarser alluvium (mainly river-deposited boulders and pebbles) forming the piedmont terrain (Central Ground Water Board, 2011). These coarse deposits are highly porous and allow for streams to flow easily underground thus allowing for extensive recharge of groundwater from the perennial rivers in the area. As a result, groundwater is unconfined and the water table is deep at 30 meters or beyond (Central Ground Water Board, 2011). The aquifers in this area are capable of yielding 100-300 m^3/hour of water (Central Ground Water Board, 2011).

Terai Belt: Adjacent to the Bhabar Belt, the Terai Belt spans across Haryana, middle to upper Uttar Pradesh, Bihar, and upper West Bengal. The region consists of newer alluvium and is characterized by fine-grained sediments from the many rivers in the area (Central Ground Water Board, 2011). The geological structure of the Terai is highly porous and permeable thus the area has access to extensive groundwater resources. This results in an upper unconfined aquifer and a lower interconnected system of confined aquifers. Tubewells here report yields of 50-200 m^3/hour of water (Central Ground Water Board, 2011).

Central Ganga Plain: Lying south of the Terai, the Central Ganga Plains contains perhaps the most productive aquifer system in India (Central Ground Water Board, 2011). Channel deposits and continuous flooding of the Ganges River creates a clastic, unconsolidated layer which hosts a widespread, multi-layered aquifer system underneath. The aquifer thickness varies from place to place, and range from a few meters to upwards of 300 meters. Though the aquifers are locally separated, they form a regional, hydraulically connected network (Karanth, 1987). Well yields here are typically in the 90 – 200 m^3/hour range (Central Ground Water Board, 2011).

4. DATA AND METHODS

This thesis makes full use of remote sensing, land surface modelling, and ground-based observations to fulfil the research objectives. A short summary of the primary datasets and the CGWB-derived GWS solution is described in Table 4.1. The individual datasets and their respective pre-processing are detailed below.

4.1. GRACE-Derived Terrestrial Water Storage

As described in Section 2.3.1, GRACE Level-3 (1° x 1°, Monthly Resolution) Terrestrial Water Storage (TWS) Release-05 (RL-05) data product from the Jet Propulsion Laboratory (JPL) for January 2003 to December 2012 is used in this work. Level-3 GRACE products have all undergone major processing to correct for errors in certain spherical harmonics and post-glacial rebound. Spatial smoothing and destriping filters have further been applied to the data product (Landerer & Swenson, 2012; Swenson & Wahr, 2006). The final output is expressed as TWS anomalies (in cm of equivalent water thickness) with respect to the average over January 2004 to December 2009. TWS anomalies during missing months have been gap filled using linear interpolation. The GRACE Level 3 solutions and the derivative data products listed below were all downloaded through GRACE TELLUS ("GRACE Land Mass Grids (Monthly)," 2013).

4.1.1. Land Grid Scaling

The previously mentioned filtering and de-striping operations are instrumental in reducing noise and removing certain correlated errors but also lead to loss in signal strength. To restore the geophysical signal, a 1° x 1° dimensionless, scaling coefficient grid is provided which needs to be multiplied with the corresponding land TWS grid (Landerer & Swenson, 2012). The scaled TWS anomaly is computed in the following manner:

$$G'(x, y, t) = G(x, y, t) * S(x, y) \tag{4.1}$$

$G(x, y, t)$ represents each unscaled grid node, x represents the longitude index, y is the latitude index, t is time (month) index, and $S(x, y)$ is the scaling grid.

4.1.2. Error Handling

In addition to the land scaling grid, measurement and leakage error grids are also provided by GRACE TELLUS. These grids are also 1° by 1° in spatial resolution and are expressed in cm of equivalent water thickness. Measurement errors are due to inaccuracies inherent in the determination of the

gravity field (Wahr, Swenson, & Velicogna, 2006) whereas leakage errors are residual errors after filtering and rescaling (Landerer & Swenson, 2012). An important statistical property of these errors is that they are generally found to be normally distributed (Wahr et al., 2006) thus the total error in TWS for a given pixel can be computed as:

$$Total\ TWS\ Error = \sqrt{Measurement_{Error}{}^2 + Leakage_{Error}{}^2} \quad (4.2)$$

4.2. GLDAS Land Surface Models

In this study, the hydrological outputs from NOAH, MOSAIC, CLM, VIC land surface models (LSM) were all used in order to counter any bias inherent in a single model. Further information on the basic schematics behind each individual land surface model is described in the Appendix. All land surface model outputs are expressed as monthly 1° x 1° grids and were available at Goddard Earth Sciences (GES) Data and Information Services Centre (DISC) ("Goddard Earth Sciences Data and Information Services Center," 2013). Soil moisture, snow-water equivalent (SWE), and canopy storage output variables were extracted for each LSM. The total soil moisture, SWE, and canopy storage can be aggregated to provide an approximation for terrestrial water storage. Thus, the LSM-derived TWS can be expressed as:

$$\Delta TWS_{GLDAS} = \Delta SM + \Delta SWE + \Delta CWS \quad (4.3)$$

Subsequently, equation 2.2 can be rewritten as:

$$\Delta GWS = \Delta TWS_{GRACE} - \Delta TWS_{GLDAS} \quad (4.4)$$

Further information on the individual land surface models, soil layer characterization, and description of hydrological variables is available in the Appendix I.

4.2.1. Anomaly and Uncertainty Expression

It is imperative that the GLDAS-derived TWS values are expressed in the same format as the GRACE-generated TWS data products. In that respect, the following computation is done for each grid pixel to generate the GLDAS-TWS anomalies with reference to the 2004-2009 mean:

$$\Delta TWS_{Anomaly}(x,y,t) = TWS_{GLDAS}(x,y,t) - \overline{TWS_{GLDAS}^{2004\rightarrow2009}}(x,y) \quad (4.5)$$

Where at each grid location, $\Delta\mathrm{TWS}_{\mathrm{Anomaly}}$ is the GLDAS-derived TWS anomaly with respect to the 2004-2009 average, $\mathrm{TWS}_{\mathrm{GLDAS}}$ is the calculated GLDAS-derived TWS value, $\overline{TWS_{GLDAS}^{2004\rightarrow2009}}$ is the average TWS value for the 2004-2009 period, x is the longitude index, y is the latitude index, and t is the time index.

Table 4-1: Primary and Secondary Source Datasets

Dataset	Units	Type	Spatial Resolution	Temporal Resolution	Observation Period	Source
JPL Level 3 TWS	EWT-cm	GRACE Observation	1°	Monthly	Jan 2003 – Dec 2012	GRACE Tellus
NOAH/ MOSAIC/ VIC/CLM Soil Moisture	Kg/m² (mm)	GLDAS Land Surface Model Parameter	1°	Monthly	Jan 2003 – Dec 2012	GIOVANNI-GLDAS
NOAH/ MOSAIC/ VIC/CLM Snow Water Eqivalent	Kg/m² (mm)	GLDAS Land Surface Model Parameter	1°	Monthly	Jan 2003 – Dec 2012	GIOVANNI-GLDAS
NOAH/ MOSAIC/ VIC/CLM Canopy Storage	Kg/m² (mm)	GLDAS Land Surface Model Parameter	1°	Monthly	Jan 2003 – Dec 2012	GIOVANNI-GLDAS
***In Situ* Well Data**	Depth to Well (m)	CGWB Observation	Point	Variable (mostly quarterly)	Variable (range from 2002 – 2012)	CGWB
CGWB-Derived GWS over U.P.	EWT -cm	Processed CGWB GWS	1°	Quarterly	March 2003 – Dec 2012	Self

The final monthly $\Delta TWS_{Anomaly}$ was derived as the average of the land surface model outputs from NOAH, MOSAIC, VIC, CLM; and the monthly error was estimated to be the standard deviation of the TWS anomalies generated from the four land surface models (Kato et al., 2007).

4.3. *In Situ* Well Data

Well depth data for 3697 wells distributed unevenly across the states of Punjab, Rajasthan, Delhi NCR, and Uttar Pradesh was made available to us in the form of Excel sheets. Time series data for the well depths varied radically from well to well in terms of temporal gaps, missing data, and number of observations. As a result, extensive pre-processing of the well time series was required to select a suitable well subset that can be used to derive the groundwater storage time series. Unfortunately, there was virtually no metadata from which to identify the aquifer type (unconfined, semi-confined, or confined), extent of land use or anthropogenic impact to the local water table, or specific yield information at each well site. Furthermore, the area is quite large and any kind of validation efforts would have to be intelligently targeted in order to infer meaningful results. To that extent, selective validation of the CGWB data over a basin or small region was carried out where there is sufficiency of high-quality well data, relatively simple hydrogeology, and heavy reliance on groundwater. Uttar Pradesh (U.P.) fulfilled the aforementioned criteria so validation of GRACE results was carried out over this region. The following sections below describe the pre-processing steps needed to convert the well depths over U.P. into groundwater storage time series. This workflow can be further visualized in Figure 4.1.

4.3.1. Quality Control Mechanism

High-quality well sites were short-listed according to the following quality control workflow:

1) Look for and remove any well records containing missing or invalid data.
2) Select only those wells that contain at least four (4) yearly observations during 2003-2012. Furthermore, there must be at least one (1) well record for each quarter (January-March, April-June, July-September, October-December).

The final output of this quality control process yielded a total of 160 wells (out of 3697) clustered mostly in southern Rajasthan and in central Uttar Pradesh. See Figure 4-2.

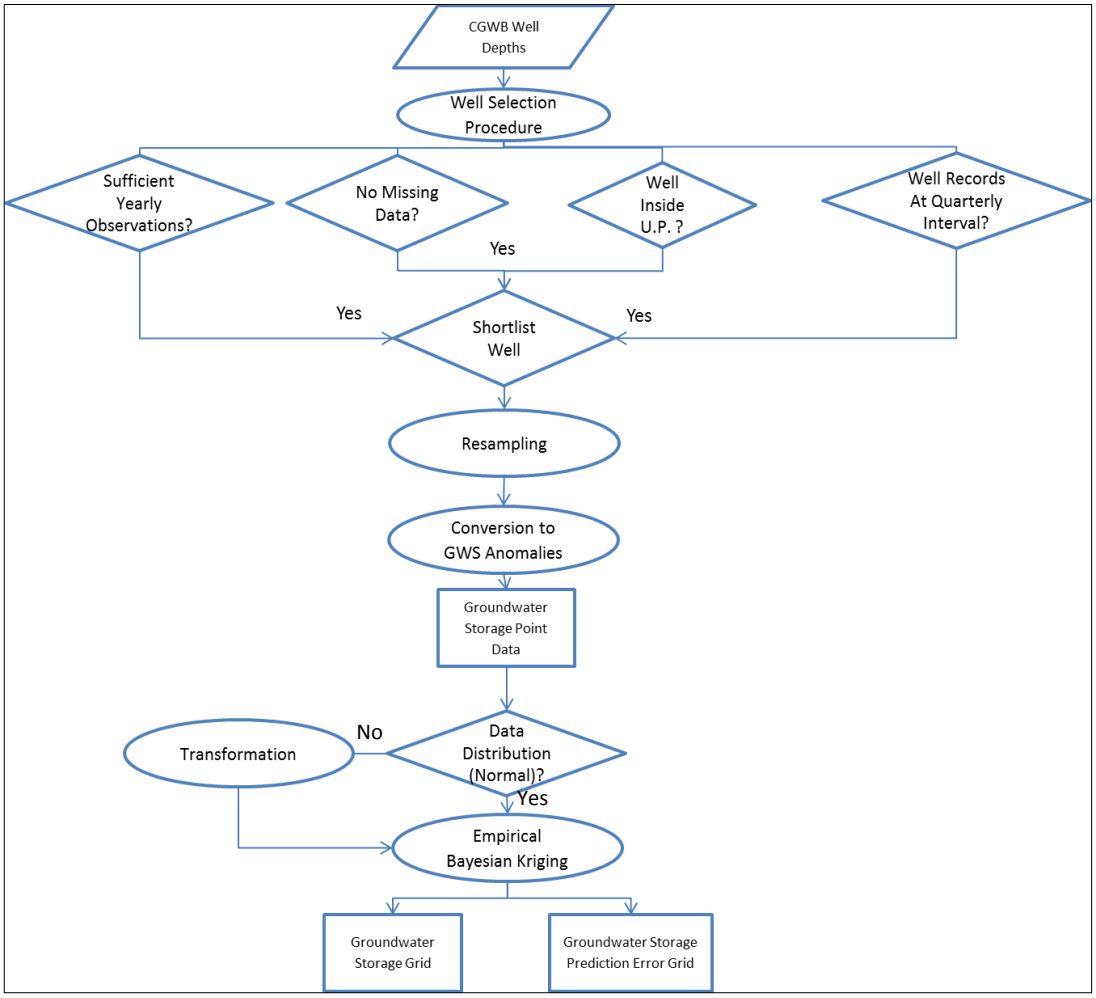

Figure 4-1: Well Data Processing Workflow

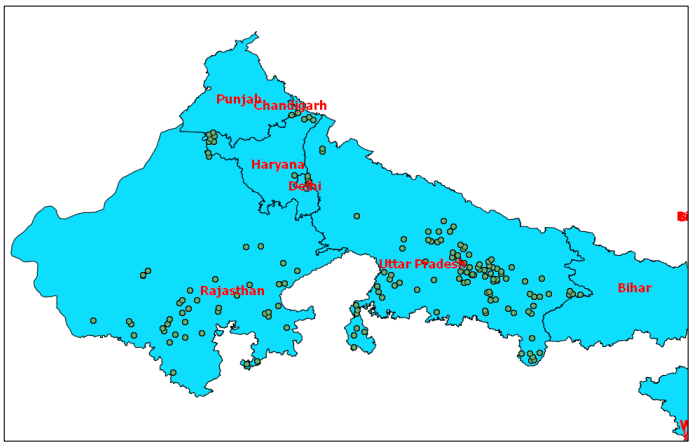

Figure 4-2: Location of Short-Listed Wells

4.3.2. Well Time Series Resampling

The final, short-listed well locations vary in temporal resolutions with most wells being measured roughly at quarterly intervals but during different months. To exacerbate matters, a few wells also record well depths at monthly intervals on certain years. It was decided that derivation of monthly well levels using regression or similar method would not be justified given the large temporal gaps in most well observations. Furthermore, the GRACE data products are recorded at monthly intervals thus it is necessary to harmonize both datasets for effective comparison. Consequently, both datasets were resampled at quarterly frequency by taking the mean well depth every three (3) months. However, the irregularity in well observations and different measurement periods signify that the resampled CGWB well data is only a rough approximation of the actual quarterly well depth at each site.

The corollary of this resampling also extends to the GRACE solution because it also needs to be resampled at quarter intervals in order for validation to ensue.

4.3.3. Selection of Validation Region

Even a casual glance at Figure 4.1 would suggest that the majority of short-listed wells are located in Uttar Pradesh and southern Rajasthan. Furthermore, the hydrogeological map of India shown in Figure 3.3 illustrates the relatively complex hydrogeology of south Rajasthan with its various scattered consolidated formations and aquifers located in hilly areas. In contrary to Rajasthan, Uttar Pradesh demonstrates a relatively simple hydrogeology with the majority of the wells localized in the Central Gangetic Plains aquifer region. Analysis of groundwater levels in Uttar Pradesh – no doubt challenging – is still easier than the interpretation of groundwater data in the hydraulically intricate South Rajasthan. Additionally, Uttar Pradesh is the most populous state in India, and has an extensive and thriving industrial and agricultural base compared to arid, sparsely populated South Rajasthan. Thus, wells in Uttar Pradesh were only considered for validation of GRACE results. Consequently, the 99 wells located in UP were further analysed.

4.3.4. Computation of Groundwater Storage Fluctuations

a) Conversion of Well Levels into Anomalies

The GRACE-derived GWS data product is expressed as equivalent heights of water relative to the 2004 to 2009 mean for that grid location. In order to harmonize the *in situ* data further with the GRACE results, the raw well depth observations for each well was converted into changes in

water table heights relative to the 2004 to 2009 mean for that well location. The calculation can be understood as:

$$\Delta H_{WTQ} = Depth_Q - \overline{Depth_{2004 \rightarrow 2009}} \quad (4.6)$$

Where ΔH_{WTQ} is the change in well level with respect to the 2004 to 2009 mean for quarter Q, $Depth_Q$ is the well depth for quarter Q, and $\overline{Depth_{2004 \rightarrow 2009}}$ is the average well level during 2004-2009. The above parameters are expressed in units of centimetres.

b) Determination of Groundwater Storage Changes from Well Level Anomalies

Under the assumption that the well measurements represent unconfined, static water table conditions (California Department of Water Resources, 2013), the groundwater storage change for each quarter can be calculated as:

$$\Delta GWS_Q = S_y \Delta H_{WTQ} \quad (4.7)$$

Where S_y is the specific yield and ΔH_{WTQ} is the change in water table height relative to the 2004 to 2009 mean for that specific quarter. This same methodology was used by Rodell et al., 2006 to derive GWS values from well data in Mississippi River Basin and by McGuire, 2009 for the High Plains Aquifer. Here, the assumption was made that the observation wells are directly linked to unconfined aquifer systems, or unconfined outcroppings of confined aquifer networks. This assumption holds true in the Terai belt in North U.P. but it is hard to verify in the central and southern U.P. which hosts a complex, multi-faceted aquifer system. To complicate matters, the presence of a large tubewell-based irrigation system in the area strongly increases the possibility of direct anthropogenic manipulation of the water table thus ensuring that the measured well depths are not static. Without adequate metadata, the effect of pumping or backflow is hard to determine. Consequently, this represents a source of error when using the equation but as an approximation, equation 4.7 will suffice.

Another point of contention involves the determination of specific yield values at each well site. The specific yield is a measure of the average storativity of an aquifer and represents the amount of water released or stored per unit change in the water table height (California Department of Water Resources, 2013). S_y values are dimensionless and are influenced by a host of factors ranging from aquifer sub-surface structure to water quality. Hence, specific yield values are site-specific. However, detailed specific yield values were not available for any of the well locations thus an extensive review of CGWB literature was carried out. For Uttar Pradesh, the specific yield values range from 0.08 to 0.18 but without further local information, it was assumed that S_y for

each well was 0.13 or the middle value. This is a major source of uncertainty as even a small mischaracterization of specific yield values can lead to serious mismatches with GRACE results (Rodell et al., 2006). For example, a $\pm$ 0.04 error would lead to a 50% change in computed GWS for a well that has a S_y of 0.08.

The two sources of uncertainty discussed so far – temporal undersampling and inaccuracy of specific yield estimates – have not been properly accounted for due to their inherent difficulty. It is hoped that these errors – if unbiased – will be smoothed out over a region (Rodell et al., 2006). The uncertainties associated with conversion of well observations into GWS are listed below in Table 4-2.

Table 4-2: List of Uncertainties When Calculating GWS for *In Situ* Well Data

Uncertainties Associated With Converting Well Depths into GWS Anomalies	
Uncertainty regarding nature of aquifer – confined or unconfined?	Temporal Undersampling
Extent of pumping and irrigation backflow – water table not static?	Mischaracterization of Specific Yield

4.3.5. Gridding of Groundwater Storage Anomalies Using Empirical Bayesian Kriging

So far, the *in situ* GWS anomalies are expressed as point shapefiles. In order for meaningful validation to take place with GRACE-derived GWS results, however, the CGWB-based GWS values have to be gridded to 1° X 1° resolution. Several interpolation schemes exist to generate a continuous surface from discrete data points and can be categorized into two different process categories: deterministic and geostatistical. Deterministic processes such as inverse distance weighing use mathematical functions to predict and fit values at unsampled locations. Geostatistical processes, or kriging, are based on probabilistic models which incorporate spatial autocorrelation (statistical relationships among measured points) when making predictions (Krivoruchko, 2011) . More importantly, these predictors are capable of quantifying the uncertainty associated with the interpolated results. As previously mentioned, errors listed in Table 4-2 have not been properly accounted for but at least with kriging, errors due to spatial undersampling can be computed and used in error propagation calculations. Due to its ability to provide standard prediction errors and its successful track record in hydrogeological applications, kriging was chosen as the interpolation method to grid the *in situ* GWS anomalies.

A more detailed description of kriging is provided in elsewhere by many authors (Goovaerts, 1997; Kitanidis, 1997). The core principle behind kriging is the use of a semivariogram to capture the spatial dependence among neighbouring observations. The variogram, $\gamma(h)$, is calculated as half of the average squared difference of all measured point pairs separated by distance h like the following:

$$\gamma(h) = \frac{1}{2N(h)} \sum_{i=1}^{N(h)} [Z(x_i) - Z(x_i + h)]^2 \quad (4.8)$$

Where $Z(x)$ represents the variable amount measured (GWS anomalies in this case), and $N(h)$ is the total number of point pairs separated by distance h. The main function of the semivariogram is to determine the weight assigned to an observed sample point when predicting new values at unmeasured locations. The empirical semivariogram generated, however, is not mathematically continuous at all separation distances and directions. In order to (i) generate a continuous prediction surface across all sampled and unsampled locations, and (ii) ensure that only positive variances are calculated; a model or a mathematically continuous curve is fitted to the empirical semivariogram (Krivoruchko, 2011). Many models exist for semivariogram fitting (spherical, circular, exponential etc.) however determination of the best model for accurate interpolation often requires extensive interaction with the data. Moreover, classical kriging assumes that the semivariogram model chosen represents the true semivariogram of the data which is rarely true in practice (Krivoruchko, 2012). To overcome the limitations of classical kriging, Empirical Bayesian kriging (EBK) was used for interpolating and gridding GWS anomalies from in *situ* data.

Empirical Bayesian kriging's main advantage over classical kriging lies in its automation of the more problematic and tedious parts of fitting the best model to the empirical semivariogram (Krivoruchko, 2012). This is achieved through a series of subsets and simulations which generate a spectrum of semivariograms in the following manner (Krivoruchko, 2012):

1) Partition the data into multiple overlapping subsets and make an initial estimation of the semivariogram at each subset.
2) The initial semivariogram model is used to simulate new data points at each input location in the subset.
3) A new semivariogram model is estimated from the simulated data. A weight for this semivariogram is then computed using Bayes' rule which indicates the likelihood that the simulated variogram will reproduce the original dataset.
4) Steps 2 and 3 are repeated a set number of times, and the initial semivariogram estimated in step 1 is used to simulate a new set of data at the input locations. The simulated data is used to estimate a new semivariogram model and its weight.

Once the above process is complete, the resultant distribution of semivariograms is used to predict values at unsampled locations. Simulated semivariograms from subsets close to the prediction location are assigned higher weights than subsets that are located far away. Below, short descriptions of the EBK model, Gaussian transformation, and model parameters are provided.

a) Kriging Model

The kriging model used for EBK is as follows (Krivoruchko, 2011):

$$\gamma(h) = Nugget + b|h|^{\alpha} \tag{4.9}$$

Where the $Nugget$ and b (slope) are positive, h is separation distance between point pairs, and α is a power factor that ranges between 0.25 and 1.75. The slope and power parameters are estimated using Bayes' rule, and the semivariogram model corresponds to a random walk process which consists of steps in a random direction that filters out a moderate trend in the data. This feature is a major improvement over classical kriging where the input dataset had to be manually detrended prior to the interpolation process.

b) Transformation

One of the primary principles behind kriging is that the input datasets adhering to a Gaussian distribution yields the best prediction. If the observation data respects a non-Gaussian distribution, it is necessary to transform the original process to a Gaussian process (Goovaerts, 1997) for optimal prediction. Fortunately, the Empirical Bayesian Kriging method embedded in the *Geostatistical Analyst* toolkit in ArcGIS 10.1 can normalize the observation data and back-transform it dynamically when carrying out the iterative kriging process.

c) Parameter Setup

In order to provide better prediction characteristics, the parameters provided in the EBK package in ArcGIS 10.1 needs to be adjusted. The most important parameter is the *Number of Simulations* (default of 100) which generates the number of semivariograms that are to be used to build the weighted prediction model that forms the cornerstone of EBK. The *Overlap Factor* (default of 1.0) is a parameter that affects the smoothness of the interpolated output, and the *Subset Size* (default of 100) determines the number of points in each subset, and also affects the number of subsets formed. The parameter configuration is detailed in the Appendix.

4.3.6. Cross-Validation and Prediction Errors

EBK, like other kriging methods, allow for the computation of prediction errors associated with the predicted surfaces. These errors are calculated through a statistical method called cross-validation which is similar to the jackknifing process (Tukey, 1958) used in statistics. Cross-validation is an accuracy assessment procedure where one data point is removed, and the remaining observation points are used to predict the value at the omitted point. The difference between the actual and predicted values are then compared and tracked. The above procedure is carried out for each of the 99 well observations in the U.P. region to generate error statistics for each interpolated grid cell. These standard prediction errors were then used for error analysis but it is important to keep in mind that these errors do not reflect the true uncertainty (see Table 4-2) associated with the *in situ* GWS grids.

4.4. Software Used

- **Python**: The bulk of the processing, analysis, error propagation, and visualization of GRACE, GLDAS, and CGWB data products were carried out using the Python programming language and various packages. This project made full use of the Anaconda Distribution ("Anaconda," 2013) which bundled the following useful libraries: NumPy, Matplotlib, PANDAS, SciPy.
- **ArcGIS 10.1**: Both ArcMap and its powerful Python-based scripting tool ArcPy were used to carry out Empirical Bayesian Kriging of *in situ* well data. It was also used to create maps and visualizing groundwater fluctuations over the study region.
- **Unidata Integrated Data Viewer (IDV)**: This open-source visualization and analysis tool ("Integrated Data Viewer (IDV)," 2013) was used to load and visualize netCDF data. It was extremely useful in observing spatio-temporal data and patterns.

4.5. Methodology

The approach used for studying interannual behaviour of groundwater in the study area is shown in Figure 4.3. The individual pre-processing procedure of the GRACE, GLDAS, and CGWB data sets was described earlier in this chapter. Building on the previous methodology, the GWS time series is calculated using equation 4.4 and trend analysis is carried out both before and after deseasonalization of the time series. Once trend analysis is complete, the deseasonalized time series is detrended to isolate the variability of the groundwater system. The interannual standard deviation is then computed at the pixel level and 12-month moving standard deviation/skewness/kurtosis is carried out over the deseasonalized, detrended GWS solution to detect shifts in interannual variability of groundwater. The same procedure is carried out for the regionally averaged GWS time series. Throughout this entire process, error propagation is carried out at every level using both first-order approximations and Monte Carlo simulations. Finally, the CGWB-

derived GWS time series is validated with the GRACE solution over Uttar Pradesh to test the agreement between GRACE and *in situ* results.

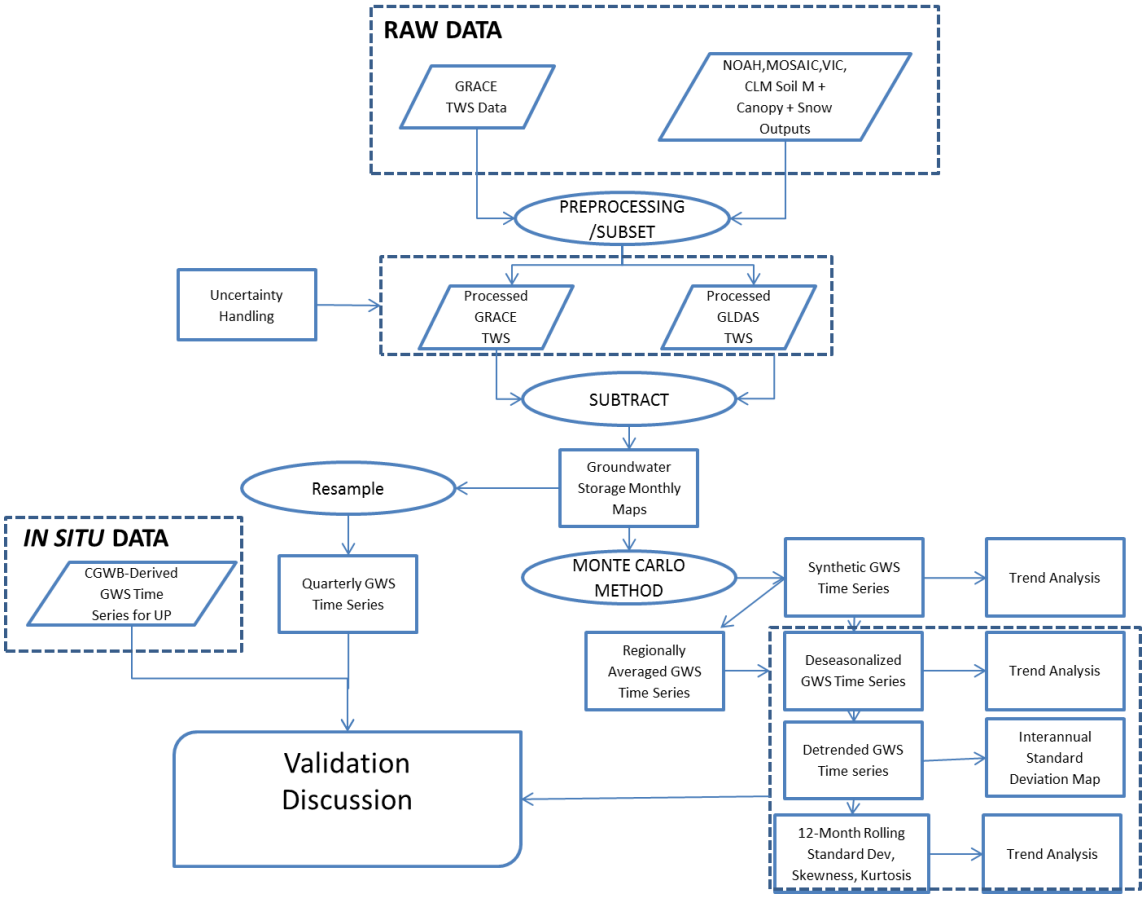

Figure 4-3: Flow chart describing overall methodology

4.5.1. Study Area Masking

The study area's shape precludes it from fitting perfectly with the GRACE and GLDAS 1° x 1° grids. One has two options when confronted with this type of problem: (i) understand that there will be some overlap with areas that are not part of the study area and accept that over a regional scale, this leakage will smoothen out, or (ii) use prior knowledge of the study area to downscale the groundwater storage in overlapping pixels to estimate the GWS contained in the study area only, and assign this estimate to that pixel value in question. Since downscaling of GWS estimation over pre-defined areas is beyond the scope of this work, the first course of action was chosen. The resulting study area mask includes some areas which extend partially into Pakistan, Nepal, Bangladesh, Jharkhand, Madhya Pradesh, and Gujarat. However, the vast majority of the overlapping pixels still lie within the Indo-Gangetic plains thus making this study area mask valid for studies in the region. See Figure 4-4 below.

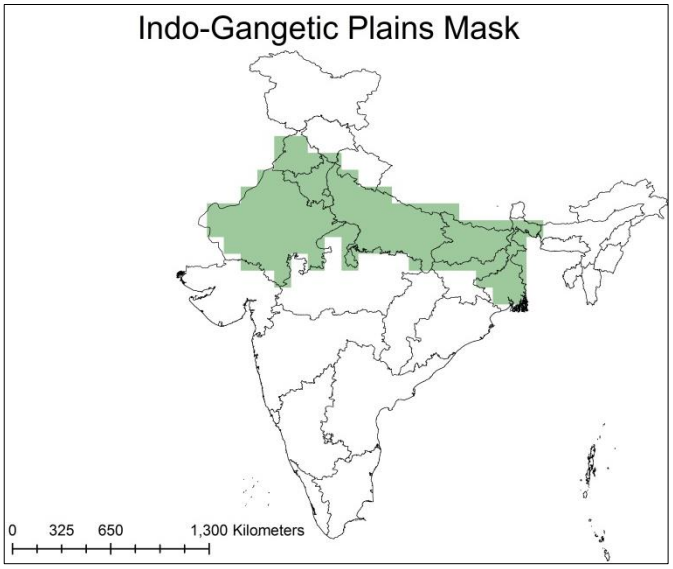

Figure 4-4: Study Area Mask

4.5.2. Deseasonalization

Meaningful interpretation of interannual groundwater variability requires removal of shorter-term signals that may distort or exaggerate the analysis. Thus, the computed GWS time series needs to be seasonally adjusted before interannual fluctuation analysis can take place. The classical decomposition technique developed by Brockwell & Davis, 2002 is used in this work to deseasonalize the GWS series. The following steps were followed assuming a monthly seasonal cycle:

1) Run a centred 12-month moving average filter over the GWS time series to approximate the trend function $\widehat{m}_t$ where t represents the time index.

2) Detrend the data by subtracting the trend function $\widehat{m}_t$ from the GWS data.

3) For each month m, calculate the average of the corresponding detrended values to obtain the *raw monthly average* s_m where $m = 1,2,\dots,12$. Another important assumption behind this seasonal index is that $s_m = s_{m+12}$.

4) The seasonal model assumes that the *raw seasonals* (or monthly averages in this case) add up to zero so that the *adjusted monthly average* $\hat{s}_m$ can be computed as:

$$\hat{s}_m = s_m - \frac{1}{12}\sum_{i=1}^{12} s_i, \qquad m = 1,2,\dots,12 \tag{4.10}$$

5) Now, the seasonality can be removed by subtracting the *adjusted monthly average* from the original GWS time series for each corresponding month to get the deseasonalized GWS time series $DGWS(t)$ where t is the time index such that:

$$DGWS(t) = GWS(t) - \hat{s}_t \tag{4.11}$$

4.5.3. Trend Analysis

A straight line was fit over the GWS time series using least-squares fitting both prior to and after deseasonalization to measure the rate of groundwater depletion (or rise). Seasonality can often distort the underlying secular trend so it is important to deseasonalize the GWS time series and then carry out trend fitting. Similarly, trends were fitted through the moving standard deviation, skewness, and kurtosis of the detrended, deseasonalized GWS time series in order to detect any shifts in groundwater variability.

4.5.4. Detrending

The secular trend in the GWS time series can interfere with and thus affect the calculation of variability measures. Thus, it is essential that the GWS data solution is detrended prior to variation analysis. In this study, least-squares fitting was used to fit a simple straight-line through the GWS time series. The aforementioned straight line was then subtracted from the deseasonalized GWS time series to detrend the data.

4.5.5. Regional Averaging

It has already been mentioned that GRACE observations only hold value over 'basin-sized' areas over 200,000 square kilometres. Thus, the GWS time series needs to be averaged over the entire region to produce meaningful results. To calculate the regional mean GWS anomaly for each month, cosine weighted means of the latitudes were used in order to compensate for meridian convergence where pixel sizes decrease toward high latitudes proportional to the cosine of latitude (Gleisner, 2011):

$$\overline{GWS}_{month} = \frac{\sum_{i=1}^{nPixels} \cos(lat_i) GWS_i}{\sum_{i=1}^{nPixels} \cos(lat_i)} \tag{4.12}$$

Where $nPixels$ represents the number of pixels in the study region, lat_i is the latitude value at a specific pixel i, and GWS_i is the GWS value at a particular pixel i.

4.5.6. *In Situ* Validation

Accuracy assessment of GRACE results was carried out by fitting a linear function to the *in situ* results, and calculating the resulting R-Squared. The R-Squared is an example of a goodness-of-fit criterion and measures the extent of variance that the fitted model (straight line) is describing. This study additionally calculated the RMS error and Pearson's Correlation Coefficient between both the GRACE and CGWB groundwater solutions. Unfortunately, as mentioned before in Table 4-2, the *in situ* data has several inherent uncertainties. The RMS error, in this circumstance, will therefore be quite a conservative measure of accuracy. Pearson's coefficient will demonstrate how well both data solutions line up and move together. Ideally, a perfect validation would yield an R-Squared of 1, RMS Error of 0, and Pearson's Coefficient of 1.

4.5.7. Error Analysis

Based on the errors of the GRACE TWS and GLDAS TWS, the error in GWS was estimated, using first-order error propagation rules, as:

$$\sigma_{GWS} = \sqrt{\sigma_{GRACE}^2 + \sigma_{GLDAS}^2} \tag{4.13}$$

Where σ_{GRACE} is the error associated with the GRACE-monthly TWS and σ_{GLDAS} is the GLDAS-monthly TWS. After this straight-forward computation, a Monte Carlo approach similar to the one used by Tiwari et al., 2009 was carried out to generate 2500 monthly synthetic GWS data sets. These synthetic GWS time series were each populated with values randomly selected from a population of Gaussian-distributed numbers $N(\mu_t, \sigma_t)$ where μ_t is the GWS value at time t and σ_t is the error is GWS at time t. This approach assumes that errors are uncorrelated from month to month which is indeed quite a questionable assumption, however Wahr et al., 2006 have remarked that the errors computed in this manner are relatively simple and realistic error figures for the current scenario. Therefore, the reader is advised to view the error and uncertainties presented in this work as a benchmark rather than a rigorous indicator of uncertainty.

Similar care needs to be presented when discussing errors in the kriging process. The standard prediction errors generated during the kriging process are primarily representative of errors in the prediction process and spatial undersampling, and are do not incorporate other inherent errors. As a result, the errors presented in this work are underestimated but have value nonetheless as a relative indicator of degree of confidence. Consequently, the standard prediction error is taken as σ_{well} where one can be fairly certain – circa 68% certain – that the predicted GWS value is within one σ_{well} of the actual GWS value. The same Monte Carlo approach described in the previous paragraph was taken here to generate synthetic time series for *in situ* GWS data.

In this study, trend fitting, time series decomposition, moving statistics, and regional averaging was carried out for each synthetic GWS data set. The resulting distribution of results was assessed, tested for normality using Jarque-Bera Test (see Appendix) or were approximated with a normal distribution, and the mean and standard deviation of the simulated results were presented respectively as the new resultant outputs and uncertainties.

5. RESULTS AND DISCUSSION

This chapter discusses the results obtained in the course of this research. The section begins with the illustration of the GWS time series and their comparison with previous works carried out by Rodell et al., 2009 and Tiwari et al., 2009. The next part deals with quantifying the interannual standard deviation of GWS over the study region and its implications. Subsequently, the topic of shifts in GWS variability is presented and its potential consequences are explored. Finally, the comparison of *in situ* and satellite-derived GWS time series over a sub-region of Uttar Pradesh is discussed.

Readers who would like to skip the discussion and just want a quick tabular summary of the results can go directly to section 5.4 titled 'Trend Analysis Comparison and Regional Statistics'.

5.1. Groundwater Storage Time Series

As mentioned before in Chapter 2, GRACE results can only be confidently applied for 'basin'-level areas occupying 200,000 km² or more. Thus, regionally–averaged GWS time series were determined for the Indo-Gangetic Plains region, Northwest India region (roughly corresponding to the Indus River Basin side of India), and the Gangetic Basin (Uttar Pradesh, Bihar, West Bengal).

5.1.1. Indo-Gangetic Plains

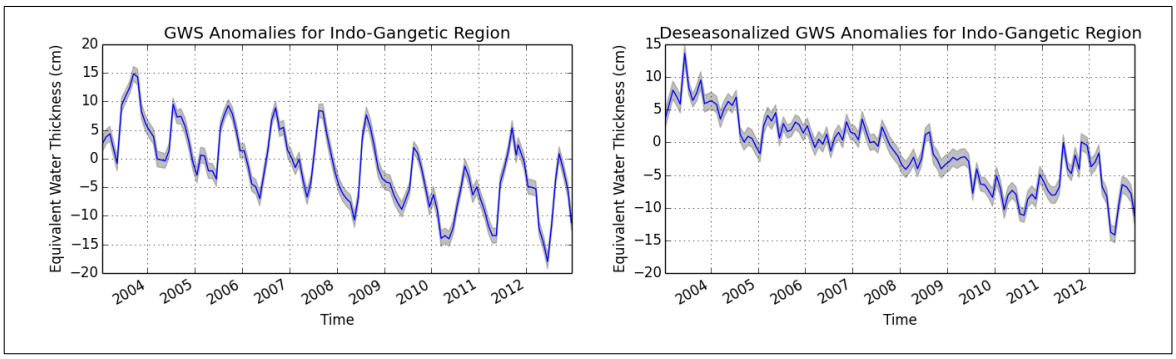

Figure 5-1: (Left) The raw regional GWS anomalies over the Indo-Gangetic Plains, and (Right) The deseasonalized GWS anomalies over the same region. The *grey shaded areas* represent the uncertainty range of the value.

Figure 5-1 shows both the regionally averaged raw and deseasonalized GWS time series over the Indo-Gangetic plains region along with their respective associated uncertainties. The raw and deseasonalized groundwater storage depletion trend was found to be $-1.5 \pm 0.04\ cm\ yr^{-1}$ and $-1.6 \pm 0.04\ cm\ yr^{-1}$. The study mask roughly covers an area of 1,000,000 km² which corresponds to a yearly depletion rate of 16 km³ yr⁻¹ (160 km³ over the 10-year period). Assuming a regional specific yield value of 0.15 (Central Ground Water Board, 2012), the regional rate of water table decline can be approximated as around -11 cm yr⁻¹ or a net lowering of the water table of 110 cm over the decade. The act of deseasonalization reduced the range of the amplitudes of the original GWS time series, and

suppressed the effect of seasonal behaviour of the original. There was, however, little effect on the determination of the overall GWS depletion trend between both time series.

The 2003-2012 time period does show a strong depletion trend in GWS that is of great concern to current regional water and food security studies. This fact has already been established elsewhere (Gleeson et al., 2012; Matthew Rodell et al., 2009; Tiwari et al., 2009). However, there have been some interesting new findings from this study that should be of more than academic interest to researchers working with GRACE data. The areas bordering the Himalayas in Figure 5-2 show the strongest depletion trends. By Occam's razor, one can use the simplest theory to explain this phenomenon: anthropogenic groundwater exploitation is most pronounced in what corresponds to the Bhabhar and Terai belt. However, this naïve assertion lacks explanatory power as this region is marked by under-utilized groundwater development due to rural poverty and poor infrastructure (Shah et al., 2006). A more plausible explanation might be attributable to extensive mass wasting and erosion taking place in the Bhabhar Belt and Shivalik Hills due to a combination of deforestation (Ramsay, 1987), landslides and debris flows (due to the rugged topography and slope instability), agricultural development, tectonics, heavy rainfall, and fluvial action (Singh, 2007). The complex interplay of these factors serves to often accelerate erosion. For example, rainfall acts a as a transportation medium to carry away sediments and weathered material but can also trigger landslides which generate enormous amounts of erosion. Similarly, tectonics may (or may not) distort the resultant GWS values as crust thickening is known to take place in the zone of interest. Thickening of the crust leads to immense generation of heat which weakens the underlying crust, resulting in vertical transport of less dense rock material upwards and consequently a negative gravity anomaly (Avouac, 2003). However, tectonic activity is also a leading catalyst for landslides which generate enormous amount of sediments which are often transported away by fluvial action. Thus, the GWS depletion signal might be exaggerated by large-scale erosion and sediment transportation at the Himalayan foothills.

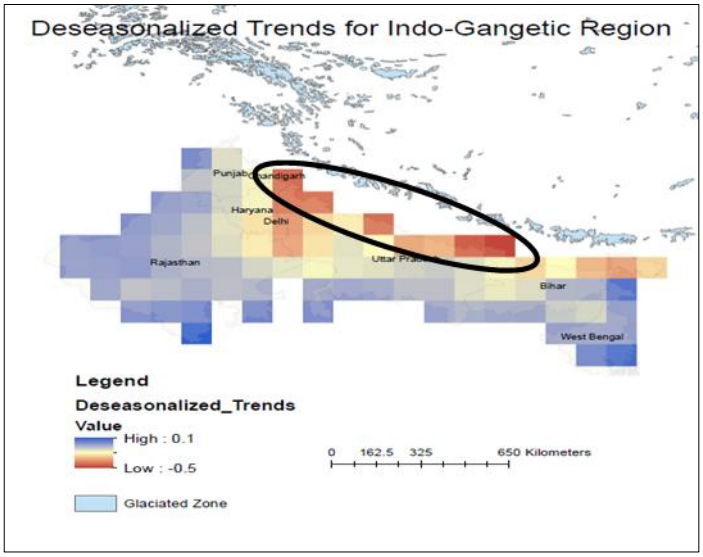

Figure 5-2: Deseasonalized Trend Map of Indo-Gangetic Region with Anomalously High GWS Depletion Rates Concentrated near the Himalayan Collision Zone

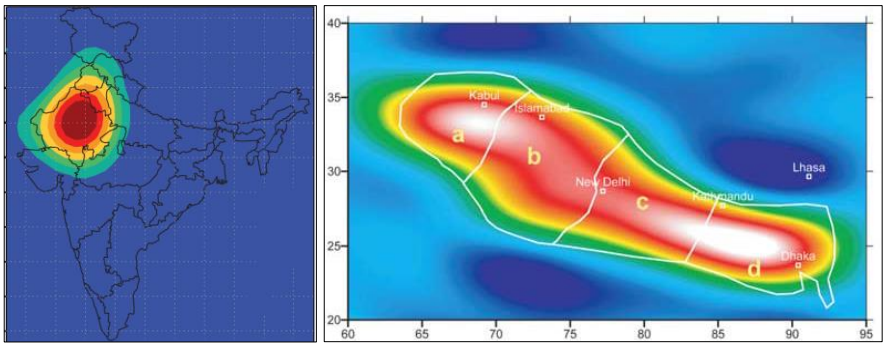

Figure 5-3: (*Left*) Study mask in Rodell's analysis for Northwest India (Rodell et al., 2009) and (*Right*) Regional subdivisions in Tiwari's work with areas c and d considered for inter-comparison (Tiwari et al., 2009)

5.1.2. Northwest India

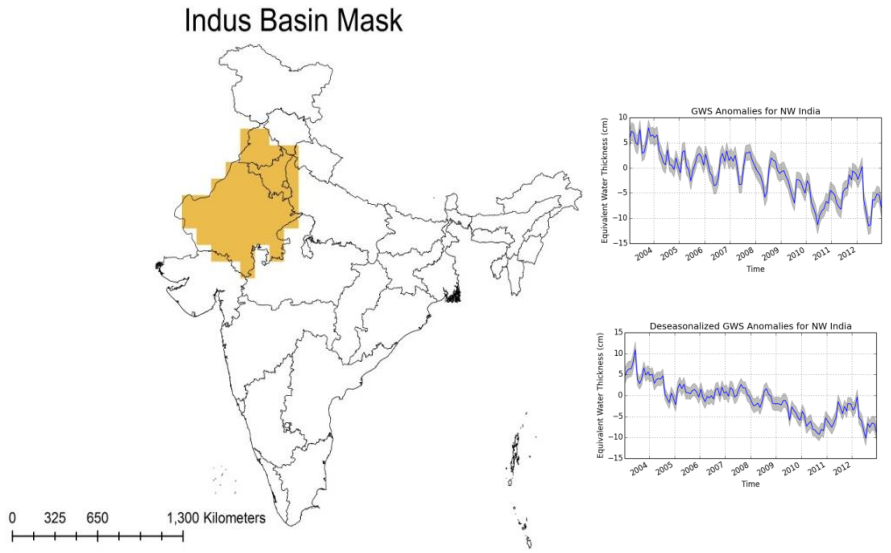

Figure 5-4: (*Left*) The Indus Basin mask used to generate the regionally averaged GWS time series for NW India. (*Upper Right*) Raw GWS anomalies and (*Upper Left*) Deseasonalized GWS anomalies for the Indus Basin region with grey area representing uncertainty range.

Rodell et al. published a paper in 2009 on the rate of groundwater depletion over Northwest India which approximately covered the states of Rajasthan, Punjab, and Haryana (including Delhi NCR). This region is underlain by the Indus River plain aquifer which is an unconfined-to-semiconfined porous alluvial formation (Rodell et al., 2009) that extends into Pakistan, India, and parts of China. A mask was created to cover roughly the same region (see Figure 5-4) and calculate the regionally averaged GWS time series over the Indus basin. Rodell and his associates estimated that there was a depletion rate of $-4.0 \pm 1.0\ cm\ yr^{-1}$ for this area from August 2002 to October 2008. In comparison, this work estimates a deseasonalized GWS depletion rate of $-1.2 \pm 0.05\ cm\ yr^{-1}$ (the raw GWS trend is extremely close to the deseasonalized GWS trend) for the same study area over the period covering January 2003 till December 2012. The study mask has a rough area of 481,000 km^2 which translates roughly into 6 km^3/yr (or 60 km^3 over the 10-year period) of groundwater storage loss. Assuming a specific yield of 0.12 (Central Ground Water Board, 2012), the Indus Basin experienced water table decline of -10 cm yr^{-1} or a net lowering of the water table of 100 cm over the 10-year period. Since this study considers a different and longer measurement period in addition to a dissimilar spatial subsetting mask (see Figure 5-3), differing GWS trend estimations were expected. However, there is a sharp difference between the trend computed by Rodell and the one computed during the course of this research. Though there was appreciable depreciation in GWS levels in the Indus Basin region, our work suggests that the depletion of groundwater has slowed down considerably. On a darker note, the results may also suggest that previously accessible groundwater reserves have mostly been tapped out, and the depletion rate has been arrested by technical and economic limitations of having to drill deeper to access existing groundwater reserves.

5.1.3. Ganga Basin

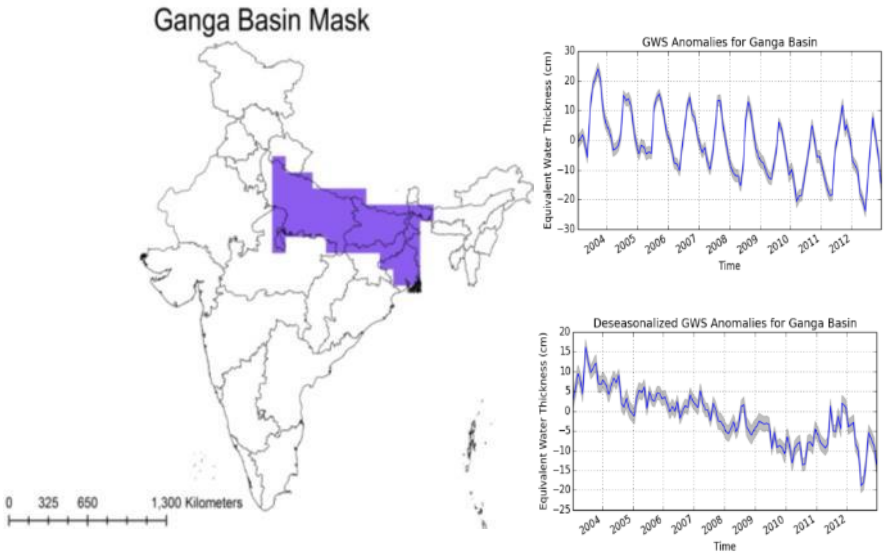

Figure 5-5: (*Left*) The Ganga Basin mask used to generate the regionally averaged GWS time series for the Central and Lower Ganges basins. (*Upper Right*) Raw GWS anomalies and (*Upper Left*) Deseasonalized GWS anomalies for the Ganges Basin region with grey area representing uncertainty range.

Tiwari et al. independently published a paper regarding dwindling groundwater resources in Northern India roughly the same time as Rodell and his team. The former's work consisted of estimating groundwater depletion across a region stretching from the Pamir Mountains in Northern Afghanistan to the Ganges-Brahmaputra Delta in Bangladesh (see Figure 5-3). Tiwari's analysis approximates the groundwater depletion rate taking place in the Gangetic-Brahmaputra basin (regions c + d) during April 2002 – June 2008 to be about 34 $km^3\ yr^{-1}$. The mask used in this study (see Figure 5-5), however, only delineates the Ganga basin and does not extend into Bangladeshi borders. Furthermore, the study period considered in this work differs from the one carried out under Tiwari and his fellow researchers. This research found heavy seasonality in the Gangetic region vis-à-vis the Indus Basin with the unprocessed, raw GWS depletion trend to be $-1.7 \pm 0.06\ cm\ yr^{-1}$. The act of seasonal adjustment provided a corrected GWS depletion trend of $-1.9 \pm 0.06\ cm\ yr^{-1}$. Since our Ganga Basin mask roughly covers an area of 521,000 km^2, the deseasonalized depletion trend translates approximately into 10 $km^3\ yr^{-1}$ (or 100 km^3 over the 10-year period) of water loss. Assuming a specific yield of 0.18 (Central Ground Water Board, 2012), the Ganges Basin experienced water table decline of -11 cm yr^{-1} or a net lowering of the water table of 110 cm over the 10-year period. Despite the areal and temporal differences between the two previous study area masks, our study suggests a large reduction in the GWS abstraction rate. A major problem associated with the GWS values in the Gangetic region consists of anomalous GWS time series values present near the Himalayas. Without filtering or accounting for these irregular leakages, it is hard to properly assess the groundwater values present in the Ganga basin.

5.1.4. Discussion

This study suggests a perceptible lowering of groundwater storage across the Indo-Gangetic plains though the recent results imply that groundwater depletion rates have decelerated considerably from their 2002-2009 estimates as established by Rodell and Tiwari. Possible reasons behind this slowdown may range from effectiveness of water conservation policies to techno-economic limitations of having to drill deeper to tap new groundwater resources. More research has to be carried out to unearth the causes for this shift in pumping behaviour. Even then, the loss of 16 $km^3\ yr^{-1}$ of groundwater over a 10-year period suggests that 160 km^3 of water has been drained from the region. To compare, the active capacity of the largest surface water reservoir in India – the Indirasagar Dam – is approximately 9.75 km^3 (Central Water Commission, 2009). Furthermore, the Ganga basin shows a steeper depletion rate than the Indus basin even though there is some concern regarding distortion of the GWS time series by external agents.

5.2. Interannual Standard Deviation

5.2.1. Indo-Gangetic Plains

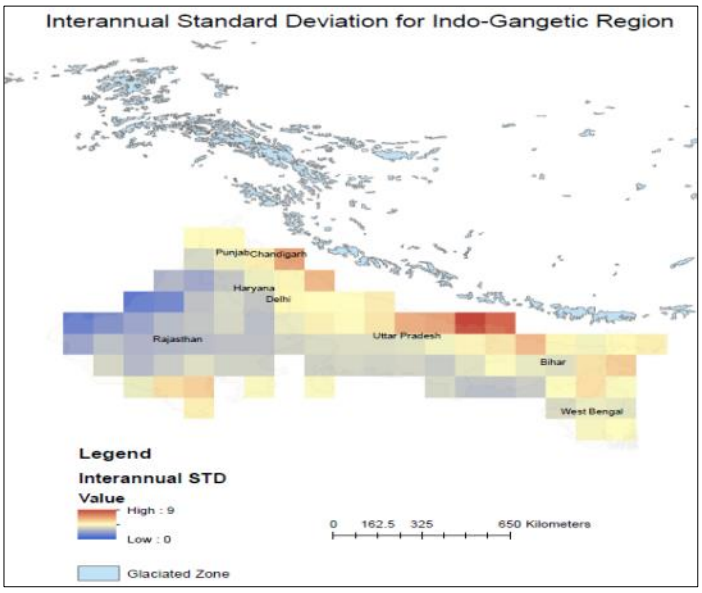

Figure 5-6: Interannual Standard Deviation Map of Indo-Gangetic Region

Figure 5-6 demonstrates a wide range of interannual variability in mean yearly GWS levels across the study region. Again, one cannot help but note that areas of high variability are concentrated along the Himalayan boundary. On a regional level, the interannual standard deviation was computed to be $1.5 \pm 0.1\ cm$ for the 10-year period beginning in 2003 and ending in 2012. 10 years is indeed a short time interval for properly assessing GWS variability yet it is an excellent starting point.

It is important to make projections with strong confidence so the $\pm 2\sigma$ approach was used to estimate an interannual GWS variability estimate of ±3.4 cm [(1.5 cm + 2*0.1 cm) * 2)] for the Indo-Gangetic plains. This means that yearly average GWS values can decrease or increase by as much as 3.4 cm from the long-term average. It may not seem like much but one must be reminded that we are dealing with *yearly averages* which compress and smooth a large amount of short-term and seasonal variations into one crisp value. A ±3.4 cm change in the yearly GWS mean signifies a possible significant change in the underlying structure and range of the intrannual GWS variability. The nature of this structural change might be due to a few extreme events or a large number of small-to-medium deviations from the mean. Nevertheless, it is important to remember that a downward direction in regional yearly average GWS of 3.4 cm would mean that the entire Indo-Gangetic region may fall short of 34 km^3 of water from the "usual" yearly expectation. Now, 34 km^3 is approximately 3.5 times the active capacity of the largest dam in India, which serves to irrigate and sustain 265,000 hectares of farmland. Such a large deficit in yearly available GWS would, be distributed unevenly across the region and - if coupled with low rainfall or dryer than usual conditions - could cascade into drought conditions.

5.2.2. Northwest India

The Indus Basin region exhibited interannual standard deviation of $1.35 \pm 0.15\ cm$. For 95% confidence projection in yearly GWS levels, an interannual variability estimate of 3.3 cm was used. Now, a reduction in yearly GWS value of 3.3 cm in the Northwest Indian region would connote a groundwater storage gap of 16 km^3 compared to annual expectations. If unaccounted for, water storage institutions and authorities may struggle to cope with the shortfall and would have to work vigorously to circumvent drought conditions.

5.2.3. Ganga Basin

The densely populated and groundwater-irrigated Ganga basin was found to face interannual standard deviation of $1.83 \pm 0.18\ cm$. Using the $\pm 2\sigma$ rule of thumb, an interannual variability approximation of 4.4 cm was determined. This is quite a large deviation from the long-term yearly average and could denote a yearly GWS shortfall as large as 23 km^3. To compare, such a loss would equate to the vanishing of 2.4 Indirasagar Dam reservoirs. Consequently, the Ganges Basin faces higher likelihood of groundwater supply shocks compared to Northwest India.

5.2.4. Discussion

This study has uncovered an element of food and water security risk that may equal GWS trend analysis in importance. The interannual standard deviation, albeit calculated over a 10-year period, can provide a relatively simple indicator of GWS volatility. Furthermore, it allows for ballpark estimates of regional-level yearly GWS shortfalls which can be useful for making projections and guiding water

management decisions. Of course, this indicator has a few issues. *One*, the interannual standard deviations calculated in the course of this work should not be treated as definitive measures of groundwater variability. A much longer observation period – usually 30 years for climatological data (Wilcox & Gueymard, 2010) – is required to establish a stable long-term mean and to incorporate a wider range of hydrological behaviour. *Two*, interannual standard deviation does not determine the direction of GWS changes but is instead an indicator of its dispersal from the mean. As such, other techniques need to be used to determine the distribution and direction of GWS values.

5.3. Shifts in Interannual GWS Variability

5.3.1. Indo-Gangetic Plains

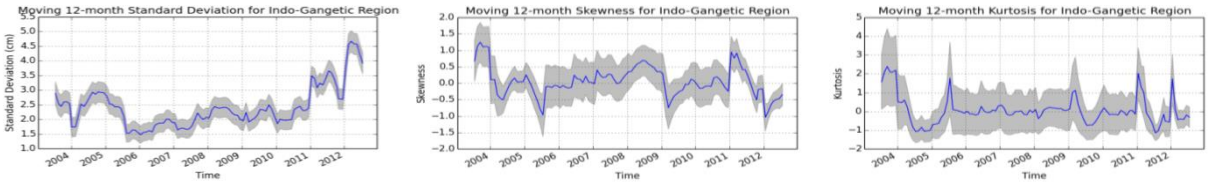

Figure 5-7: Moving Statistics for Indo-Gangetic Plains

Moving statistics plots of the regionally averaged, deseasonalized, and detrended GWS time series (see Figure 5-7) over the Indo-Gangetic plains yielded important information about the underlying structure of interannual GWS variability. First, the moving 12-month standard deviation shows rather intriguing behaviour with an uptick of $0.12 \pm 0.04\ cm\ yr^{-1}$. From the plot, it can be deduced that 12-month GWS variability as a function of time was mostly constant till late 2010 and steadily climbs upwards afterwards. Of course, 10-year is a short period in which to establish reliable variability measurements however in the vital interest of water security, one should not dismiss these findings in an off-handed manner. If anything, this phenomenon should be carefully monitored and tracked as it may point to fundamental shifts in regional groundwater dynamics. Combine the fact that the region faces net groundwater loss with the observation that GWS interannual variability is increasing in recent years, and we have a major water and food risk issue. Not only the region will face declining water tables but dealing with an increasingly erratic water table would require advanced storage and distribution mechanisms.

The interpretation of the moving skewness and kurtosis is quite difficult but shows little to no trend. The moving skewness and kurtosis trends were computed to be $-0.04 \pm 0.05\ yr^{-1}$ and $-0.06 \pm 0.09\ yr^{-1}$ with the standard errors exceeding the trends themselves thus rendering the calculated trends undependable. Statistical testing using the Jarque-Bera test of the groundwater time series over the Indo-Gangetic plains strongly suggested that the aforementioned series follow a Gaussian distribution. Since there is little to no change in the underlying skewness and kurtosis, the Gaussian nature of the GWS time

series is preserved. However, there is evidence that the standard deviation may be rising and this possibility would entail an uptick in the frequency and magnitude of extreme GWS behaviour.

5.3.2. Northwest India

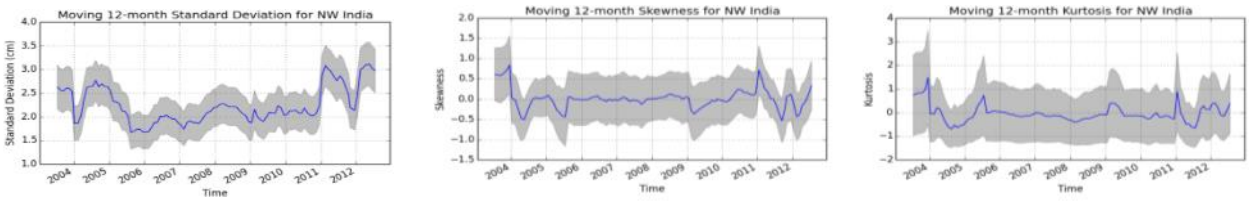

Figure 5-8: Moving Statistics for Northwest India

The 12-month moving standard deviation trend for NW India was calculated to be $0.04 \pm 0.05\ cm\ yr^{-1}$ with the error being comparable to the trend in standard deviation. The 12-month moving skewness and kurtosis trends respectively are $-0.01 \pm 0.05\ yr^{-1}$ and $-0.02 \pm 0.11\ yr^{-1}$ which are negligible and lack confidence due to the error bars being many times larger than the estimated values. Thus, no significant shifts in GWS variability were detected in Northwest India during the 10-year period.

5.3.3. Ganga Basin

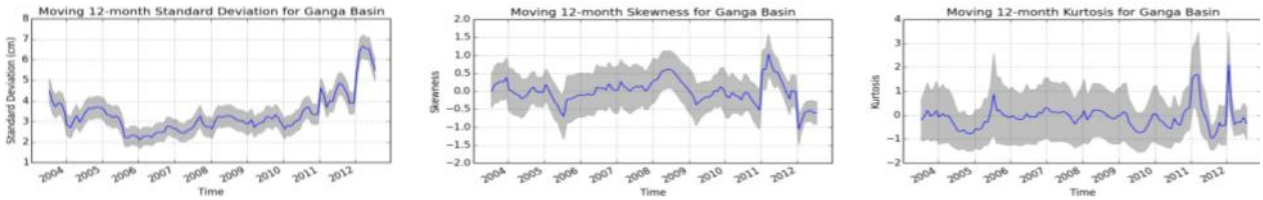

Figure 5-9: Moving Statistics for Ganga Basin

The rolling statistics for the Ganga Basin paint a far more interesting picture. With a 12-month moving standard deviation showing an increasing trend of $0.18 \pm 0.06\ cm\ yr^{-1}$, this value is higher in magnitude than the overall Indo-Gangetic regional trend. Since Northwest India shows little to no shift in variability, the majority of the overall regional variation is driven by groundwater activity in the Ganga basin. The trends in skewness and kurtosis are less significant at $-0.01 \pm 0.05\ yr^{-1}$ and $0.02 \pm 0.08\ yr^{-1}$. The moving standard deviation over the 10-year period seems to accelerate around late 2010 which is consistent with the overall regional movement in interannual GWS variability. However, there is real concern that the variability in the Ganga Basin might be driven by erosion-driven mass loss. This factor has to be studies in more detail, and a longer observation period is needed to conclusively establish any shift in interannual GWS variability.

5.3.4. Discussion

Though 10 years is quite a small observation period to study shifts in GWS variability, there is evidence to suggest that the yearly variability of groundwater is increasing over the Gangetic Basin, and over the entire Indo-Gangetic plains. Combined with a negative regional GWS trend, these results indicate not only a general lowering of the water table but a more volatile water table that needs to be managed carefully. The findings in these studies suggest not only that authorities should step up water conservation efforts but need to re-think their water storage and distribution systems in light of increasing GWS variance.

5.4. Trend Analysis Comparison and Variability Statistics

This section summarized the results obtained in sections 5.1-5.3 in a tabular format for quick summary and visualization. In Table 5-1, comparison of the GWS trend analysis between the current work and previous works is presented. Table 5-2 depicts the regional GWS parameters and statistics for the Indo-Gangetic Plains, Indus River Basin, and Ganges River Basin.

Table 5-1: Trend Analysis Comparison between Present and Previous Works

	Present Work (NW India)	***Rodell's Analysis (NW India)***	***Present Work (Ganga Basin)***	***Tiwari's Analysis (Ganga-Brahmaputra Basin)***
Observation Period	**January 2003 – December 2012**	**August 2002 – October 2008**	**January 2003 – December 2012**	**April 2002 – June 2008**
Areal Extent	**See Figure 5-4**	**See Figure 5-3**	**See Figure 5-5**	**See Figure 5-3 (only regions c and d)**
Groundwater Volume Change	**6 ± 0.2 km^3 yr^{-1}**	**17.7 ± 4.5 km^3 yr^{-1}**	**10 ± 0.3 km^3 yr^{-1}**	**34 km^3 yr^{-1}**
Water Table Decline	**0.10 ± 0.004 m yr^{-1}**	**0.33 ± 0.08 m yr^{-1}**	**0.11 ± 0.003 m yr^{-1}**	**(Not Available)**

Table 5-2: Regional Statistics Table

Regional Statistics	*NW India (Indus Basin)*	*Ganga Basin*	*Indo-Gangetic Plains*
Raw GWS Trend	-1.2 ± 0.05 cm yr^{-1}	-1.7 ± 0.06 cm yr^{-1}	-1.5 ± 0.04 cm yr^{-1}
Deseasonalized GWS Trend	-1.2 ± 0.05 cm yr^{-1}	-1.9 ± 0.06 cm yr^{-1}	-1.6 ± 0.04 cm yr^{-1}
Interannual Standard Deviation	1.35 ± 0.15 cm	1.83 ± 0.18 cm	1.5 ± 0.1 cm
Projected (95% Confidence) Yearly GWS Shortfall	16 km^3	23 km^3	34 km^3
Moving Standard Deviation Trend	0.04 ± 0.05 cm yr^{-1}	0.18 ± 0.06 cm yr^{-1}	0.12 ± 0.04 cm yr^{-1}
Moving Skewness Trend	-0.01 ± 0.05 yr^{-1}	-0.01 ± 0.05 yr^{-1}	-0.04 ± 0.04 yr^{-1}
Moving Kurtosis Trend	-0.02 ± 0.11 yr^{-1}	0.02 ± 0.08 yr^{-1}	-0.06 ± 0.09 yr^{-1}

5.5. Selected Validation of GRACE-Derived GWS in Uttar Pradesh Sub-Region

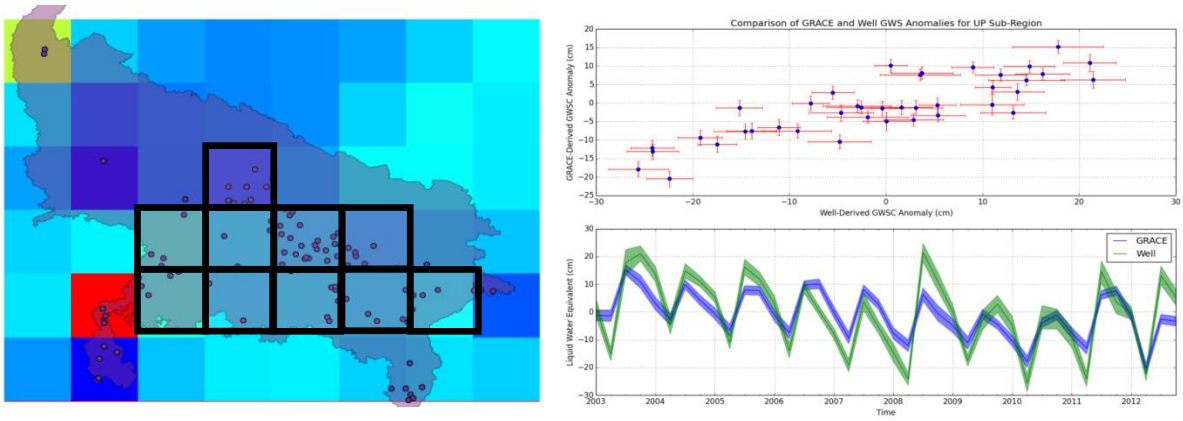

Figure 5-10: (*Left*) The map of Uttar Pradesh with purple dots showing well locations and black squares representing the study area. (*Upper Right*) Plot of regionally averaged GRACE-GWS vs. CGWB-GWS with error bars, and (*Bottom Left*) comparison of GRACE and CGWB GWS time series with shaded areas representing uncertainty.

A 10-pixel study mask was established over central and southern U.P. to cover the area containing the majority of observation wells (see Figure 5-10). The mask, unfortunately, covers roughly an area of 100,000 km^2 which is much less than the stipulated recommended area of 200,000 km^2. However, the well

distribution constrained the mask to cover merely 10 pixels. The area chosen however is not without merit as it covers a heavily populated, urbanized, irrigated, and industrialized zone.

Comparison of the regionally averaged GRACE- and CGWB-based GWS solutions was optimistic with R-Squared of 0.64 ± 0.05, RMS error of $8.43 \pm 0.53\,cm$, and Pearson's Correlation Coefficient of 0.80 ± 0.03 (see Table 5-3). First of all, the R-Squared value suggests a strong one-to-one relationship between both time series with the independent variable (*in situ* data) explaining 64% of the variation in the dependent variable (GRACE data). The remaining 36% of the variance might be attributed to misspecification of specific yields, temporal undersampling, and other unknown factors. Furthermore, both time series show very strong correlation and 'line up' for the most part. Similar work over Bangladesh (Shamsudduha et al., 2012) yielded Pearson's Correlation Coefficient of 0.93 and RMS error less than 5 cm whereas a study over Yemen resulted ijjn R-Squared of 0.79 and RMS error of 0.04 cm (Moore & Fisher, 2012). These studies all monitor wells at monthly intervals and have accurate information regarding specific yields of the aquifers. The work carried out over Uttar Pradesh has similar accuracy statistics as far as R-Squared and Pearson's Correlation are considered however RMS error is rather high in relation to GRACE validations in different parts of the world. With better information regarding specific yields and more frequent well observation, it is very likely that the gap between GRACE and CGWB results will close and better accuracy statistics can be determined.

The RMS error is quite large at 8.43 cm with the *in situ* data GWS time series showing wider range of movement than the GWS-based time series. Assuming a specific yield of 0.13, this RMS error translates to well depth differences of 70 cm and above between the GRACE and CGWB GWS datasets. This error is indeed quite large but considering the large uncertainties inherent in processing the CGWB datasets as well as the small size of the study area, surprisingly good agreement still exists between both the remote sensing and *in situ* GWS solutions.

Table 5-3: Validation Statistics

Validation Statistics	Value
R-Squared	0.64 ± 0.05
RMS Error	8.43 ± 0.53 cm
Pearson's Correlation Coefficient	0.80 ± 0.03

6. CONCLUSION AND RECOMMENDATIONS

6.1. Conclusion

On Anomalously High Groundwater Depletion Rates along the Eurasian-Indian Plate Collision Zone

An interesting result encountered in this study – based on the GRACE and GLDAS-derived results – is that the highest rate of groundwater abstraction takes place along the Himalayan foothills where the Indian and Eurasian plates converge. This study hypothesizes that the GWS values along the Himalayas are altered by possible tectonics and erosion-driven mass loss. Future work should concentrate on removing or diminishing the impact of these processes for better TWS and GWS calculations.

On Uncertainty Propagation

This study does not purport to be an authoritative nor even a formal study of GRACE-related errors and error propagation. The uncertainties provided in this work are not to be taken as rigorous indicators of error but as reasonable degrees of confidence. As such, the Monte Carlo simulations presented here are simplistic and brute force simulations which assume that measurements are not temporally correlated (which are rarely the case). The resulting simulations often followed a Gaussian distribution but when this was not the case, a Gaussian function was fitted to the distribution in order to approximate the average output value and its associated standard deviation (uncertainty). Thus, one must take care to interpret the uncertainties provided in this study with the typical $\pm 2\sigma$ 95% confidence interval approach. Still, as a rough approximation of the error, the uncertainties listed here are sufficient.

On the Rate of Groundwater Depletion in North India

Compared to previous studies carried out by Rodell and Tiwari, the rate of groundwater depletion has reduced significantly over the period 2003-2012. The reason behind this slowdown in depletion may be due to a variety of factors which may range from optimistic (better water conservation and management policies, better awareness of extent of water resources) to the pessimistically practical (the easy-to-reach aquifers have been mostly tapped out, and economic/technical limitations – at the moment – prevent further exploitation of deeper groundwater reserves). Nevertheless, this study estimates that there still was a net loss of 160 km^3 of water during the study period over the Indo-Gangetic plains. To put this number into perspective, this approximation is equivalent to more than sixteen (16) times the active capacity of the largest dam reservoir in India. Unchecked extraction of groundwater reserves at this rate will still lead to serious water and food security repercussions in the region.

The study estimated the GWS depletion taking place separately in Northwest India (roughly corresponding to the Indus River Basin) and the Ganges Basin with the conclusion that depletion is more pronounced in the Ganges basin. However, the correctness of this assertion has to be further verified pending correction for possible anomalous GWS values along the Himalayan region. Even then - assuming that the leakage is smoothed out when carrying out regional averaging – the spotlight falls on the Gangetic basin as a hotspot for groundwater depletion vis-à-vis the Indus basin. Historically, this part is known to face lower agricultural productivity and poorer infrastructure. Now, burdening this region with large-scale, unsustainable groundwater abstraction will render a poor, vulnerable region even poorer and more vulnerable.

On Interannual Standard Deviation as an Indicator of Water Risk

This study introduced a relatively straight-forward to measure the yearly variability of groundwater storage at regional scales using the concept of interannual standard deviation. It is now possible to get a rough approximation of the extent of 'worst-case' shortfall in GWS that a region might face even though there might be little to no long-term net loss of water. Using the $\pm 2\sigma$ approach, this study estimated that the Indo-Gangetic plains may fall short of 34 km^3 of groundwater in a year compared to the expected 'long-term mean.' Now, this is a large amount of water (equivalent to almost 3.5 Indirasagar dams) and though its effects will be distributed over a large geographical locale, areas lacking adequate water storage and distribution mechanisms will face the full brunt of this hydrological shock. Of course, the estimates provided in this work reflect a rough approximation and should be treated conservatively. Usually, observation periods of 30 years or more are used to capture the full range of hydrological behaviour, and our 10-year time series is frankly too short a period. Furthermore, the extent of groundwater variability is only useful in relation with the readiness of the water storage and distribution infrastructure to absorb such shortfalls. Consequently, the usefulness of the interannual standard deviation can only be intelligently assessed in relation to the strength of the water storage/distribution infrastructure. Still, this work can be used as a starting point for new water security studies that focus on water storage and distribution. Groundwater depletion can and should be combatted with robust water conservation practices, but an erratically behaving groundwater system may require stronger storage and distribution mechanisms.

The interannual standard deviation was found to be larger in Ganges Basin than the Indus River basin. Assuming that leakage from non-groundwater sources has been mostly ironed out; this point is a matter of grave concern for the Ganges basin. The region not only faces comparably (to NW India) higher groundwater depletion but also has to contend with more volatile groundwater levels. This problem can only then be effectively combatted with a combination of robust water conservation and storage/distribution mechanisms.

On Possible Shifts in Interannual GWS Behaviour

Though 10 years is admittedly a very short period in which to assess shifts in GWS behaviour, this work has uncovered a non-negligible increasing trend in the 12-month moving standard deviation of the interannual GWS time series. Whether this is an artefact of the shorter observation period is not yet clear, but the evidence collected during the course of this work suggests that variability of GWS is on the rise in Indo-Gangetic plains. If anything, this behaviour should be closely monitored as shifts in variability may serve as precursors to a sweeping transformation of the entire regional groundwater system. As the range of water levels become more unpredictable, the region has to strongly consider upgrading its existing storage and distribution systems. The GWS values were found to follow a Gaussian distribution, and ensuing moving skewness and kurtosis showed little to no trend thus suggesting that the underlying distribution of the GWS retained its Gaussian nature. However, the upward tick in the moving standard deviation suggests that there is an increase in variability of the GWS with portends frequent and higher magnitude extreme behaviour in groundwater storage.

Interestingly, Northwest India shows no discernible change in interannual GWS variability but the Gangetic basin shows a non-negligible change in moving standard deviation. This suggests that the large part of the shift in variability in GWS in the region is driven by groundwater dynamics in the Ganges Basin. A strong caveat: it is yet unclear how much of the variability in groundwater storage in Ganges Basin is propelled by possible leakage of tectonics and erosion in the Himalayan region.

On Validation of GRACE-Derived GWS over a Sub-Region in Uttar Pradesh

In the absence of adequate metadata, the conversion of *in situ* well observations into gridded GWS values required undertaking several assumptions. For example, it was presumed that each short listed well was connected to an unconfined aquifer, and all had the same specific yield. These assumptions, combined with temporal undersampling and heterogeneity, added a large element of uncertainty to the final GWS outputs but the comparison with GRACE-derived solutions was still agreeable. Both GWS solutions are strongly correlated and show a strong linear one-to-one relationship. Though the RMS error was on the high side and a small sized sub-region was chosen, both datasets – regardless of their uncertainties – mostly 'lined up' and showed similar behaviour. Having more detailed metadata and more frequent observations – which is often difficult in India – would help immensely in establishing more accurate GWS values and bring more definitive comparison between *in situ* and GRACE-based GWS datasets.

Final Thoughts

The combination of a net loss of groundwater and a rise in GWS variability paint a bleak picture heralding not only large-scale water scarcity but also wide-ranging volatility in water tables. Instead of despairing, however, this work hopes to be a catalyst for young and old minds alike to tackle these formidable challenges by tapping our deepest reservoirs of creativity, imagination, and perseverance. This study does

not aspire to be a pessimistic one. If anything, groundwater depletion rates have slowed down remarkably compared to previous estimates and GRACE now can be used to make projections regarding yearly shortfalls of regional groundwater storage. With these remote sensing tools and better foresight of the regional groundwater dynamics, the future of North India does not have to be a water stressed one.

6.2. Recommendations

General Recommendations

- Study and better identify the possible leakage of tectonics and erosion-driven mass loss into pixels of interest. A method needs to be discovered which limits or eliminates this effect from leaking into terrestrial water storage solutions.
- In this study, brute force is used in Monte Carlo simulations to generate thousands of synthetic time series by randomly generating GWS values from a Gaussian distributed population. It is more prudent to use stratified random sampling (such as latin hypercube sampling) in order to choose less but more meaningful samples in order to cut down on computational processing power and storage considerations.
- Studies of GWS or climatological variability need observation periods lasting 30 years or more. If possible, 30 years of *in situ* well data should be procured and the method of interannual standard deviation and moving statistics needs to be carried out in order to test the validity of the approach presented in this work.
- Carry out validation of GRACE data over a region exceeding 200,000 km^2 with wells containing adequate metadata regarding specific yield information and aquifer properties.
- Statistically downsample GRACE-derived results to finer spatial resolutions while ensuring that error bars are kept at a minimum in order to make GRACE data useful at the state and local scale.
- Provided that GRACE-derived GWS results can be successfully downsampled, overlay ancilliary information such as population, food access, demographics, water access etc. to better assess water risk. In this way, the projected shortfall in yearly GWS can be compared to existing water storage/distribution infrastructure before a risk score can be assigned.
- Explore possible links between GRACE-based GWS time series and climatic teleconnections such as El Nino-Southern Oscillation, Indian Ocean Dipole, and other phenomena that operate at interannual time scales.

Recommendations Aimed at Policymakers

- This study indicates that groundwater depletion rate has slowed down significantly compared to the studies carried out by Tiwari and Rodell which is an excellent turn of events. The government must continue and strengthen existing water conservation measures which encourage artificial recharge of aquifers, suspension of non-critical pumping if water table reaches critical depths etc.

- Besides water conservation policies, policymakers should review the existing water storage and distribution systems in light of the possibility of increased variability in GWS and to account for projected shortfalls in groundwater storage.
- Irrigation is the major consumer of groundwater in the region yet the water delivery and routing infrastructure is often inefficient. Increasing the efficiency of existing irrigation systems would go a long way in reducing groundwater depletion rates.
- The GRACE satellite system is projected to lose functionality by 2015 or 2016 ("GRACE Orbit Lifetime Prediction," 2011). The world has never seen an observation system like this and its loss will be a major blow to hydrological and scientific research worldwide. A continuation of the GRACE satellite re-using the same satellite design and concept will be more than satisfactory in extending the vital work carried out by the GRACE system.
- Currently, the information embedded in GRACE data solutions is woefully untapped. Policymakers can help in this regard by encouraging and funding further research and tinkering with GRACE data and products. They may be surprised by the insight that can be gained from such ventures.

REFERENCES

Aggarwal, P. K., Joshi, P. K., Ingram, J. S. I., & Gupta, R. K. (2004). Adapting food systems of the Indo-Gangetic plains to global environmental change: key information needs to improve policy formulation. *Environmental Science & Policy*, *7*(6), 487–498. doi:10.1016/j.envsci.2004.07.006

Ahmadi, S. H., & Sedghamiz, A. (2006). Geostatistical Analysis of Spatial and Temporal Variations of Groundwater Level. *Environmental Monitoring and Assessment*, *129*(1-3), 277–294. doi:10.1007/s10661-006-9361-z

Anaconda. (2013). Continuum Analytics. Retrieved from https://store.continuum.io/cshop/anaconda/

Avouac, J.-P. (2003). Mountain building, erosion, and the seismic cycle in the Nepal Himalaya. *Advances in Geophysics*, *46*, 1–80.

Booth, E., Mount, J., & Viers, J. H. (2006). Hydrologic variability of the Cosumnes River floodplain. *San Francisco Estuary and Watershed Science*, *4*(2). Retrieved from http://escholarship.org/uc/item/71j628tv.pdf

Brockwell, P. J., & Davis, R. A. (2002). *Introduction to time series and forecasting* (Vol. 1). Oxford, UK: Taylor & Francis.

California Department of Water Resources. (2013). *Calculating Annual Change in Groundwater Storage Using Groundwater Level Data*. Sacramento, CA. Retrieved from http://www.waterplan.water.ca.gov/cwpu2013/index.cfm

Central Ground Water Board. (2012). *Aquifer Systems of India* (Government). New Delhi. Retrieved from http://cgwb.gov.in/AQM/

Central Ground Water Board, Ministry of Water Resources, Government of India. (2011). *Dynamic Ground Water Resources of India (as of 31 March 2009)*. Faridabad, India.

Central Water Commission. (2009). *India: National Register of Large Dams*. New Delhi.

Chandramouli, C. (2011). Population, Size, and Decadal Change. In *Primary Census Abstract* (Vol. Data Highlights). New Delhi: Census of India.

DeCarlo, L. T. (1997). On the meaning and use of kurtosis. *Psychological Methods*, *2*(3), 292.

Delbari, M., Motlagh, M. B., Kiani, M., & Amiri, M. (2013). Investigating spatio-temporal variability of groundwater quality parameters using geostatistics and GIS. *International Journal of Applied and Basic Sciences, 4*(10), 3623-3632.

Doane, D. P., & Seward, L. E. (2011). Measuring skewness: a forgotten statistic. *Journal of Statistics Education*, *19*(2), 1–18.

Folland, C. K., Karl, T. R., & Jim Salinger, M. (2002). Observed climate variability and change. *Weather*, *57*(8), 269–278.

Gleeson, T., Wada, Y., Bierkens, M. F. P., & van Beek, L. P. H. (2012). Water balance of global aquifers revealed by groundwater footprint. *Nature*, *488*(7410), 197–200. doi:10.1038/nature11295

Gleisner, H. (2011). *Latitudinal Binning and Area-Weighted Averaging of Irregularly Distributed Radio Occultation Data* (No. 10). Danish Meteorological Institute.

Goddard Earth Sciences Data and Information Services Center. (2013). NASA. Retrieved from http://disc.sci.gsfc.nasa.gov/

Goovaerts, P. (1997). *Geostatistics for natural resources evaluation*. Oxford, UK: Oxford University Press.

Goswami, R. (2014, February 14). System to Monitor Groundwater. *The Telegraph*. Calcutta, India. Retrieved from http://www.telegraphindia.com/1140214/jsp/northeast/story_17933558.jsp#.UxRidvmSxnY

GRACE Land Mass Grids (Monthly). (2013). GRACE Tellus. Retrieved from http://grace.jpl.nasa.gov/data/mass

GRACE Orbit Lifetime Prediction. (2011, December 2). University of Texas Center for Space Research. Retrieved from http://www.csr.utexas.edu/grace/operations/lifetime_plots/

Haile, K. H. (2011, March). *Estimation of Terrestrial Water Storage in the Upper Reach of Yellow River* (Masters). University of Twente, Enschede, NL. Retrieved from www.itc.nl/library/papers_2011/msc/wrem/habte.pdf

Hiraishi, T., Nyenzi, B., Odingi, R., Penman, J., Habetsion, S., Kruger, D., … Buendia, L. (2000). Quantifying Uncertainties in Practice. In *IPCC Good Practice Guidance and Uncertainty Management in National Greenhouse Gas Inventories* (p. 34). Kanagawa, Japan: Institute for Global Environmental Strategies.

India among high risk nations in water stress survey. (2013, December 14). *The Times of India*. Retrieved from http://timesofindia.indiatimes.com/india/India-among-high-risk-nations-in-water-stress-survey/articleshow/27341315.cms

Integrated Data Viewer (IDV). (2013, March 29). Unidata. Retrieved from http://www.unidata.ucar.edu/software/idv/

Jain, S., & Singh, V. P. (2003). Groundwater. In *Water Resources Systems Planning and Management* (pp. 235–294). Amsterdam; Boston: Elsevier.

Jarque, C. M., & Bera, A. K. (1987). A test for normality of observations and regression residuals. *International Statistical Review/Revue Internationale de Statistique*, 163–172.

Jha, B. M., & Sinha, S. K. (2009). Towards Better Management of Groundwater Resources in India. *Quarterly Journal*, *24*(4), 1–20.

Karanth, K. R. (1987). *Ground water assessment: development and management*. New Delhi; New York: Tata McGraw-Hill Education.

Kato, H., Rodell, M., Beyrich, F., Cleugh, H., GORSEL, E. van, Liu, H., & Meyers, T. P. (2007). Sensitivity of Land Surface Simulations to Model Physics, Land Characteristics, and Forcings, at Four CEOP Sites (< Special Issue> Coordinated Enhanced Observing Period (CEOP)). *Journal of the Meteorological Society of Japan. Ser. II*, 187–204.

Kitanidis, P. K. (1997). *Introduction to geostatistics: applications in hydrogeology*. Cambridge; New York: Cambridge University Press.

Kovalevsky, V. S. (1992). Trends in the long-term variability of groundwater discharge. *GeoJournal*, *27*(3), 269–274.

Krivoruchko, K. (2011). *Spatial statistical data analysis for GIS users*. Esri Press Redlands, CA, USA.

Krivoruchko, K. (2012). Empirical Bayesian Kriging: Implemented in ArcGIS Geostatistical Analyst. *ESRI*. Retrieved from www.esri.com/news/arcuser/1012/files/ebk.pd

Landerer, F. W., & Swenson, S. C. (2012). Accuracy of scaled GRACE terrestrial water storage estimates: ACCURACY OF GRACE-TWS. *Water Resources Research*, *48*(4), n/a–n/a. doi:10.1029/2011WR011453

Machiwal, D., Mishra, A., Jha, M. K., Sharma, A., & Sisodia, S. S. (2012). Modeling Short-Term Spatial and Temporal Variability of Groundwater Level Using Geostatistics and GIS. *Natural Resources Research*, *21*(1), 117–136. doi:10.1007/s11053-011-9167-8

McGuire, V. L. (2009). *Water-level changes in the High Plains aquifer, predevelopment to 2007, 2005-06, and 2006-07* (Scientific Investigations Report) (p. 9). Reston, Virginia: U.S. Geological Survey. Retrieved from http://pubs.usgs.gov/sir/2009/5019/

Mikhailov, V., Tikhotsky, S., Diament, M., Panet, I., & Ballu, V. (2004). Can tectonic processes be recovered from new gravity satellite data? *Earth and Planetary Science Letters*, *228*(3-4), 281–297. doi:10.1016/j.epsl.2004.09.035

Milich, L., & Weiss, E. (2000). GAC NDVI interannual coefficient of variation (CoV) images: Ground truth sampling of the Sahel along north-south transects. *International Journal of Remote Sensing*, *21*(2), 235–260. doi:10.1080/014311600210812

Misra, A. K., Saxena, A., Yaduvanshi, M., Mishra, A., Bhadauriya, Y., & Thakur, A. (2006). Proposed river-linking project of India: a boon or bane to nature. *Environmental Geology*, *51*(8), 1361–1376. doi:10.1007/s00254-006-0434-7

Moore, S., & Fisher, J. B. (2012). Challenges and Opportunities in GRACE-Based Groundwater Storage Assessment and Management: An Example from Yemen. *Water Resources Management*, *26*(6), 1425–1453. doi:10.1007/s11269-011-9966-z

Nahar, N., Hossain, F., & Hossain, M. D. (2008). Health and socioeconomic effects of groundwater arsenic contamination in rural Bangladesh: new evidence from field surveys. *Journal of Environmental Health*, *70*(9).

Ogawa, R. (2010). *Transient, seasonal and inter-annual gravity changes from GRACE data: geophysical modelings*. PhD Dissertation, Hokkaido University, Sapporo.

Political Map of India. (2012, June 12). Political, www.mapsofindia.com. Retrieved from http://www.mapsofindia.com/maps/india/india-political-map.htm

Rajeevan, M., & McPhaden, M. J. (2004). Tropical Pacific upper ocean heat content variations and Indian summer monsoon rainfall. *Geophysical Research Letters*, *31*(18). Retrieved from http://www.agu.org/pubs/crossref/2004/2004GL020631.shtml

Ramsay, W. J. H. (1987). Deforestation and erosion in the Nepalese Himalaya-is the link myth or reality. In *Forest Hydrology and Watershed Management, Proceedings of the Vancouver Symposium, IAHS Publ.* Retrieved from http://ks360352.kimsufi.com/redbooks/a167/167024.pdf

Reig, P., Shiao, T., & Gassert, F. (2013). *Aqueduct Water Risk Framework* (Working Paper). Washington, DC: World Resources Institute. Retrieved from http://www.wri.org/publication/aqueduct-waterrisk- framework

Restrepo, J. D., & Kjerfve, B. (2000). Magdalena river: interannual variability (1975–1995) and revised water discharge and sediment load estimates. *Journal of Hydrology*, *235*(1), 137–149.

Rodell, M., Houser, P. R., Jambor, U., Gottschalck, J., Mitchell, K., Meng, C.-J.,Toll, D. (2004). The Global Land Data Assimilation System. *Bulletin of the American Meteorological Society*, *85*(3), 381–394. doi:10.1175/BAMS-85-3-381

Rodell, Matthew, Chen, J., Kato, H., Famiglietti, J. S., Nigro, J., & Wilson, C. R. (2006). Estimating groundwater storage changes in the Mississippi River basin (USA) using GRACE. *Hydrogeology Journal*, *15*(1), 159–166. doi:10.1007/s10040-006-0103-7

Rodell, Matthew, Velicogna, I., & Famiglietti, J. S. (2009). Satellite-based estimates of groundwater depletion in India. *Nature*, *460*(7258), 999–1002.

SAS Elementary Statistics Procedure. (2008). In *SAS OnlineDoc® 9.1.3*. Cary, NC: SAS Institute Inc. Retrieved from http://support.sas.com/onlinedoc/913/getDoc/en/proc.hlp/a002473332.htm

Sehgal, V. K., Singh, M. R., Chaudhary, A., Jain, N., & Pathak, H. (2013). Vulnerability of Agriculture to Climate Change: District Level Assessment in the Indo-Gangetic Plains. New Delhi: Indian Agricultural Research Institute.

Shah, T., Roy, A. D., Qureshi, A. S., & Wang, J. (2003). Sustaining Asia's groundwater boom: An overview of issues and evidence. In *Natural Resources Forum* (Vol. 27, pp. 130–141). Wiley Online Library. Retrieved from http://onlinelibrary.wiley.com/doi/10.1111/1477-8947.00048/abstract

Shah, T., Singh, O. P., & Mukherji, A. (2006). Some aspects of South Asia's groundwater irrigation economy: analyses from a survey in India, Pakistan, Nepal Terai and Bangladesh. *Hydrogeology Journal*, *14*(3), 286–309. doi:10.1007/s10040-005-0004-1

Shamsudduha, M., Taylor, R. G., & Longuevergne, L. (2012). Monitoring groundwater storage changes in the highly seasonal humid tropics: Validation of GRACE measurements in the Bengal Basin: VALIDATING GRACE ΔGWS IN THE HUMID TROPICS. *Water Resources Research*, *48*(2), n/a–n/a. doi:10.1029/2011WR010993

Sharma, B., Mukherjee, A., Chandra, R., Islam, A., Dass, B., & Ahmed, M. R. (2008). Groundwater governance in the Indo-Gangetic Basin: an interplay of hydrology and socio-ecology. In *2nd International Forum on Water & Food*.

Sharma, B. R., Amarasinghe, U. A., & Sikka, A. (2008). Indo-Gangetic river basins: Summary situation analysis. *New Delhi, India: International Water Management Institute. Pp14*. Retrieved from http://cpwfbfp.pbworks.com/f/IGB_situation_analysis.PDF

Shum, C. K., Guo, J.-Y., Hossain, F., Duan, J., Alsdorf, D. E., Duan, X.-J., … Wang, L. (2010). Inter-annual Water Storage Changes in Asia from GRACE Data. In R. Lal, M. V. K. Sivakumar, S. M. A. Faiz, A. H. M. Mustafizur Rahman, & K. R. Islam (Eds.), *Climate Change and Food Security in South Asia* (pp. 69–83). Dordrecht: Springer Netherlands. Retrieved from http://link.springer.com/10.1007/978-90-481-9516-9_6

Singh, B. K. (2007). Assessment of the Upstream Churia Hills and Downstream Terai Plains Linkage: An Environmental Services Perspective. *Banko Janakari*, *20*(1). Retrieved from http://www.mtnforum.org/sites/default/files/publication/files/6710.pdf

Smith, E. (2006). Uncertainty analysis. *Encyclopedia of Environmetrics*. Retrieved from http://onlinelibrary.wiley.com/doi/10.1002/9780470057339.vau001/full

Swenson, S., & Wahr, J. (2006). Post-processing removal of correlated errors in GRACE data. *Geophysical Research Letters*, *33*(8). doi:10.1029/2005GL025285

Tapley, B. D., Bettadpur, S., Ries, J. C., Thompson, P. F., & Watkins, M. M. (2004). GRACE measurements of mass variability in the Earth system. *Science*, *305*(5683), 503–505.

Tiwari, V. M., Wahr, J., & Swenson, S. (2009). Dwindling groundwater resources in northern India, from satellite gravity observations. *Geophysical Research Letters*, *36*(18), L18401.

Tremblay, L., Larocque, M., Anctil, F., & Rivard, C. (2011). Teleconnections and interannual variability in Canadian groundwater levels. *Journal of Hydrology*, *410*(3), 178–188.

Tukey, J. W. (1958). Bias and confidence in not-quite large samples. In *Annals of Mathematical Statistics* (Vol. 29, pp. 614–614).

Vinnikov, K. Y., & Robock, A. (2002). Trends in moments of climatic indices. *Geophysical Research Letters*, *29*(2). doi:10.1029/2001GL014025

Wahr, J., Molenaar, M., & Bryan, F. (1998). Time variability of the Earth's gravity field: Hydrological and oceanic effects and their possible detection using GRACE. *Journal of Geophysical Research: Solid Earth (1978–2012)*, *103*(B12), 30205–30229.

Wahr, J., Swenson, S., & Velicogna, I. (2006). Accuracy of GRACE mass estimates. *Geophysical Research Letters*, *33*(6). doi:10.1029/2005GL025305

Washington, R., New, M., Hawcroft, M., Pearce, H., Rahiz, M., & Karmacharya, J. (2012). Climate change in CCAFS regions: Recent trends, current projections, crop-climate suitability, and prospects for improved climate model information. Retrieved from https://dspace.ilri.org/handle/10568/21109

What is Empirical Bayesian Kriging? (2012). In *ArcGIS Desktop Help 10.1*. ESRI.

Wilcox, S., & Gueymard, C. (2010). Spatial and temporal variability of the solar resource in the United States. *Washington, DC: NREL/DoE [National Renewable Energy Laboratory/Department of Energy]*. Retrieved from http://rredc.nrel.gov/solar/new_data/variability/Documentation/ASES_47760_final.pdf

Winter, T. C. (1999). *Ground water and surface water: a single resource* (Vol. 1139). Denver, CO: U.S. Geological Survey.

Zhang, G. P., & Qi, M. (2005). Neural network forecasting for seasonal and trend time series. *European Journal of Operational Research*, *160*(2), 501–514.

APPENDICES

Appendix - I: Land Surface Model Parameters

(Source: Rodell et al., 2004)

Table A: Physical parameters available from GLDAS

Parameter	Unit
Surface pressure	Pa
Near surface air temperature	K
Near surface wind magnitude	m/s
Near surface specific humidity	kg/kg
Total evapotranspiration	kg/m^2
Snow water equivalent	kg/m^2
Total canopy water storage	kg/m^2
Soil layer temperature	K
Soil layer moisture	kg/m^2
Snowmelt	$(kg/m^2)/s$
Net shortwave radiation	W/m^2
Net longwave radiation	W/m^2
Latent heat flux	W/m^2
Sensible heat flux	W/m^2
Snowfall rate	$(kg/m^2)/s$
Rainfall rate	$(kg/m^2)/s$
Average surface temperature	K
Ground heat flux	W/m^2
Surface incident shortwave radiation	W/m^2
Surface incident longwave radiation	W/m^2
Subsurface runoff	kg/m^2
Surface runoff	kg/m^2

Table B: Soil parametrization of the land surface models

Land Surface Models	Depths
CLM 2.0 (10 Soil Layers; 3.433 m deep)	0-0.018, 0.018-0.045, 0.045-0.091, 0.091-0.166, 0.166-0.289, 0.289-0.493, 0.493-0.829, 0.829-1.383, 1.383-2.296, and 2.296-3.433 m
MOSAIC (3 Soil Layers; 3.50 m deep)	0-0.02,0.02-1.50, and 1.5-3.50 m
NOAH (4 Soil Layers; 2.0 m deep)	0-0.1, 0.1-0.4, 0.4-1.0, and 1.0-2.0 m
VIC (3 Soil Layers; 1.9 m deep)	0-0.1, 0.1-1.6, and 1.6-1.9 m

Appendix - II: Jarque-Bera Test

(Source: Jarque & Bera, 1987)

The Jarque-Bera is a relatively straight-forward method to test whether samples could have been drawn from a normally distributed random variable. Its basic premise is to utilize the sample skewness and kurtosis to check if the sample follows a normal distribution. Ideally, a normally distributed random variable has a sample skewness of 0 and sample kurtosis of 3. The test statistic is computed as:

$$JB = \frac{n}{6}(s^2 + \frac{(k-3)^2}{4}) \quad (1)$$

Where n is the sample size, s is the sample skewness, and k is the sample kurtosis. The test statistic JB asymptotically approximates a chi-squared distribution with two degrees of freedom which can be used to construct p-values that test whether the sample is derived from a normal distribution. In this study, the null hypothesis that the sample did not follow a normal distribution was assumed to be rejected at the 0.05 level.

Appendix - III: Empirical Bayesian Kriging Parameter Setup

Source: ("What is Empirical Bayesian Kriging?," 2012)

Output raster cell size = 1.0 Degree

Transformation Type = 'EMPIRICAL' (Multiplicative Skewing transformation with Empirical base function)

Maximum Local Points = 20 (Subsets will not have more than this many points)

Overlap Factor = 1 (Degree of overlap between subsets. Higher the factor, the smoother the output but at cost of higher processing time)

Number of Semivariograms Simulated = 1000

Search Neighbourhood (Standard Circular):

Radius = 3.0 Degrees

Angle = 0

Maximum Neighbours = 15

Minimum Neighbours = 6

Sector Type = 'One Sector'

Appendix - IV: Kriging Cross-Validation Results

Table C: Error Statistics of Kriging Process

TIME	STANDARD PREDICTION ERROR	RMS
2003/03/31	7.19	7.38
2003/06/30	7.01	6.69
2003/09/30	15.5	12.8
2003/12/31	8.06	7.99
2004/03/31	7.55	7.57
2004/06/30	8.19	8.17
2004/09/30	8.26	8.34
2004/12/31	6.60	6.18
2005/03/31	6.01	6.15
2005/06/30	6.15	5.94
2005/09/30	8.42	8.63
2005/12/31	4.61	4.57
2006/03/31	4.95	5.46
2006/06/30	6.81	6.51
2006/09/30	7.62	7.70
2006/12/31	5.67	5.85
2007/03/31	5.99	5.66
2007/06/30	5.35	5.28
2007/09/30	9.18	8.99
2007/12/31	6.76	6.80
2008/03/31	7.11	6.96
2008/06/30	9.14	9.44
2008/09/30	8.31	8.64
2008/12/31	7.26	7.71
2009/03/31	6.24	6.50
2009/06/30	8.54	8.45
2009/09/30	10.1	10.1
2009/12/31	9.34	8.81
2010/03/31	6.70	6.65

2010/06/30	11.0	10.9
2010/09/30	11.3	11.3
2010/12/31	8.91	9.24
2011/03/31	9.06	9.07
2011/06/30	8.74	8.54
2011/09/30	12.6	12.2
2011/12/31	11.3	10.7
2012/03/31	10.1	9.60
2012/06/30	9.70	9.29
2012/09/30	12.1	11.5
2012/12/31	10.3	10.0